The Role of the Apparent Rate Constant of Cross-Bridge Transition From the Strong Binding State (g_{app}) in Skeletal Muscle Force Production

by

Christopher William Ward

Dissertation submitted to the Graduate Faculty of the Virginia Polytechnic Institute And State University in partial fulfillment of the requirements for the degree of

Doctor of Philosophy

in

Veterinary Medical Sciences: Physiology

APPROVED:

John C. Lee, Co-Chairman

Jay H. Williams, Co-Chairman

Ludeman A. Eng

Gary A. Klug

Charles J. McGrath

July 1, 1996
Blacksburg, Virginia

Keywords: Cross-bridges, Calcium, Contraction, Muscle, Myosin

The Role of the Apparent Rate Constant of Cross-Bridge Transition From the Strong Binding State (g_{app}) in Skeletal Muscle Force Production

by

Christopher William Ward

John C. Lee, Co-Chairman Jay H. Williams Co-Chairman

Abstract

Force regulation at the level of the actin-myosin cross-bridge (XB) can be described by a 2 state model in which the XB's cycle between a strongly bound (SB), force generating state and a weakly bound (WB), non-force generating state. This cycle can be characterized by the apparent rate constants for transition into the SB state (f_{app}) and returning to the WB state (g_{app}). Increases in XB force can be accounted for by an increase in f_{app}, a decrease in g_{app} or both. While effort towards understanding XB force regulation has focused on the notion that force production is primarily regulated by f_{app}, the purpose of this investigation was to determine if g_{app} contributes to force regulation at the XB and to determine whether g_{app} differs in muscles with differing contractile characteristics.

Specifically, g_{app} is an apparent rate constant which represents the sum of the biochemical rates which characterize the transition from the SB state to the WB state. Estimates of g_{app} were experimentally derived by determining the ratio of myosin ATPase activity to force across a physiological range of calcium (Ca^{2+}) in skinned muscle fibers. Insights into g_{app} were gained by comparing the $[Ca^{2+}]_{50}$ (concentration of Ca^{2+} required to elicit 50% of maximal force or ATPase activity) of ATPase activity and force. For example, if g_{app} contributes to XB force regulation it would be expected that g_{app} would be sensitive to increasing $[Ca^{2+}]$ which would manifest in differing Ca^{2+} sensitivities between ATPase and force.

Measurements of $[Ca^{2+}]_{50}$ for force and ATPase in fast fibers from the frog (20°C 2.0mM [MgATP]) were significantly different (2.64±0.14 vs. 1.58±0.08 μM Ca^{2+}, $p<.05$) . The separation of these curves resulted in a decreasing of A/F by nearly four fold over submaximal levels of Ca^{2+}. At maximal Ca^{2+} activation g_{app} was 2.90 s^{-1}.

To further explore the role of g_{app} in XB cycling, measurements of A/F were made at reduced [MgATP](1.0, 0.5, 0.25 mM) in frog fibers. Decreased [MgATP] would be expected to slow the SB to WB transition (breaking of the rigor bond) thus reducing g_{app}. Reduced [MgATP] resulted in progressively smaller differences in the $[Ca^{2+}]_{50}$ of force and ATPase. This lead to a reduction in the Ca^{2+} sensitivity of g_{app}.

Fast fibers are known to be less sensitive to Ca^{2+}($[Ca^{2+}]_{50}$) and contract with faster kinetics compared to slow fibers. Since differences in g_{app} should exist between muscles with differing contractile characteristics, g_{app} was examined between soleus (slow) and extensor digitorum longus (EDL, fast) fibers of the rat While no differences in F_{max} (maximal Ca^{2+} activated force) were seen between the fiber types, differences in A/F ratios were seen between both fiber types. With increasing Ca^{2+} activation, this estimate of g_{app} shows a 5.5-fold decrease in EDL fibers and a 2.5-fold decrease in SOL fibers. At maximal Ca^{2+} activation g_{app} was $3.13\pm0.35s^{-1}$ and $1.50\pm0.04s^{-1}$ for fast and slow fibers respectively.

To determine to what extent differences in g_{app} account for the differences in the $[Ca^{2+}]_{50}$ between fast and slow fibers, reductions in [MgATP] to 0.5 mM were used. Slow fibers exhibited no differences in the $[Ca^{2+}]_{50}$ between force and ATPase. In fast fibers, $[Ca^{2+}]_{50}$ of force was different at 2.0 mM, this difference was abolished at 0.5 mM [MgATP]. This suggests that differences in calcium sensitivity of force between fast and slow muscle are due in part to g_{app}.

Based on the findings that g_{app} is calcium sensitive and that altering g_{app} can alter contractile kinetics (i.e. $[Ca^{2+}]_{50}$ for force) it appears that g_{app} plays a role in the modulation of contractile characteristics at the skeletal muscle XB.

DEDICATION

I dedicate this work to my parents William and Virginia Ward. Their tireless support makes it possible for me to achieve my goals.

ACKNOWLEDGEMENTS

When reaching any personal milestone, the achievement is often put into perspective by reflecting on the journey. Time and time again I first acknowledge my parents William and Virginia Ward. Not only did they grant me a world of opportunities by adopting me, they supported me in all of my endeavors. Thank you Mom and Dad. I also am blessed with a wonderful sister who has seen me through thick and thin. Thank you LoriAnn. I also must acknowledge Susan Mullenex. Susan has been my best friend and my biggest supporter over the past three years and has truly made my life complete.

As any one who knows me well can attest, the path through my graduate education has been influenced by several people. The first is my mentor and friend Dr. Jay H. Williams. Jay has selflessly offered his time and guidance through my college education. As one of his first official graduate students I believe he has experienced the full gamut of "dealing" with a graduate student with me in his apprenticeship. The only way I could possibly repay my debt to him is to emulate him in my professional endeavors.

The second person who I must acknowledge is Dr. John C. Lee. I have not yet met a graduate student who has had the opportunity to work with Dr. Lee and not been positively influenced. I have spent numerous occasions in Dr. Lee's office seeking advice about my graduate program and have left knowing more about myself. One of my few regrets is that I did not have more opportunities to work with Dr. Lee in my tenure at VMRCVM. I truly hope that I have the opportunity to learn from him in the future.

I also acknowledge the rest of my committee members. I have truly benefited from the experience of being a doctoral student and the guidance of Dr. Ludeman Eng, Dr. Charles McGrath, Dr. Gary Klug and Dr. Tom Nosek. I appreciate all of their time and effort in shaping and reviewing my work and providing a beneficial graduate experience. I realize that upon finishing my program I am afforded the opportunity to develop into a academician and I couldn't have had any better role models.

Finally, I have had so many positive experiences with the faculty, staff and graduate students at VMRCVM, the Dept of Human Nutrition and Foods, and elsewhere at the university, that it is impossible for me to name them all. I truly could not have had the full experience of a graduate education if so many individuals had not lent me a hand, a word of encouragement, a piece of advice, or a warm welcome along the way. YOU know who you are.....Thank you.

This project was supported, in part, by a grant from the National Institute of Arthritis, Musculoskeletal and Skin Diseases, AR 41727.

TABLE OF CONTENTS

LIST OF FIGURES

LIST OF TABLES

INTRODUCTION

Skeletal muscle contraction is a voluntary process controlled by neural signals originating in the central nervous system (CNS). Nerve impulses from the CNS travel via motor neurons which synapse with a few to several hundred muscle fibers. This multi-fiber innervation results in a functional motor unit which activates the fibers in its service in an all-or-none fashion, one strategy for enabling graded neuromuscular control.

Within the muscle cell, force output results from the interaction of actin-myosin crossbridges (XB). At the XB level, force can be described by a sigmoidal relationship between free calcium (Ca^{2+}) and force production (Figure 1). In the resting cell most Ca^{2+} is sequestered in the sarcoplasmic reticulum (SR) leaving the myoplasmic concentration around 50nM. At this level of Ca^{2+} no detectable force is generated by the contractile apparatus. Increasing levels of intracellular Ca^{2+} results in increased force output until maximal force is realized at 5-10 μM Ca^{2+}. As intracellular Ca^{2+} increases, Ca^{2+} binding sites on troponin are progressively saturated until maximal force is produced. Relaxation of the system occurs when Ca^{2+} is re-sequestered into the SR.

The force-free Ca^{2+} relationship has been one of the most effective ways to examine the functional aspects of the contractile apparatus. This relationship provides general information on the contractile apparatus such as the level of Ca^{2+} needed to elicit maximal force production (F_{max}) and the Ca^{2+} sensitivity of the system. However, in order to fully understand the causative factors of the force-free Ca^{2+} relationship, one must

examine the regulation of force at the level of the XB. This becomes particularly important when one considers that alterations in the force-free Ca^{2+} curve have been used to explain differences in whole muscle force production between different fiber types (Huchet & Leoty, 1993; Gardetto, Schluter and Fitts, 1989) as well as changes in force elicited by metabolic perturbations (e.g., pH, P_i etc.) (Fabiato & Fabiato, 1978; Godt & Nosek, 1989; Metzger & Moss, 1987 and 1990; Cooke, Franks, Luciani & Pate, 1988; Donaldson & Hermansen, 1978; Cooke & Pate, 1985; Stienen, Roosemalen, Wilson & Elzinga, 1990) activity, inactivity and disease states (e.g., hypertrophy and atrophy) (Kandarian & Williams, 1993; McDonald & Fitts, 1995; Gardetto, Schluter & Fitts, 1989). Without a thorough understanding of force generation at the level of the XB, mechanisms contributing to changes in contractile apparatus function cannot be identified.

In simplified form, force regulation by the XB's can be examined as a two state model. In relaxed fibers myosin binds to actin at a rapid rate and with low affinity. This binding makes no contribution to force production but results in some fiber 'stiffness' and is considered a weak binding (WB) or non-force generating state. When Ca^{2+} is present above a threshold concentration of $\sim 10^{-7}$ M the strong binding (SB) or force producing state occurs. This latter state is characterized by an increase in myosin's affinity for actin and an increase in ATP hydrolysis which in turn provides energy for force production by myosin. Transition between these two states involves a number of biochemical steps and is described by the apparent rate constant for transition from WB into the SB state (f_{app}) and the apparent rate constant for the transition from the SB into the WB state (g_{app}).

Statement of The Problem

Brenner (1986, 1988) suggests that regulation of XB force output by this system is due to the kinetics of XB cycling between these two states such that the ratio of f_{app} and g_{app} determines force. Effort towards understanding XB force regulation has focused on the notion that force production is primarily regulated by f_{app}. Increasing f_{app} reflects increases in the fraction of XB's in the SB state which in turn increases force output by the sarcomere. While much attention has been devoted towards investigation of f_{app} and its regulation by Ca^{2+}, the rate constant governing the return to the WB state (i.e., g_{app}) has received relatively little attention. The importance of g_{app} is evident in that changes in g_{app} can affect both the shape and position of the force-free Ca^{2+} curve. For example, a decrease in g_{app} would also reflect an increase in the fraction of XB's in SB and increase force produced by the contractile apparatus.

Estimates of g_{app} can be experimentally derived by determining the ratio of myosin ATPase activity to force (A/F) across a physiological range of Ca^{2+} (Brenner 1988, 1986; Kerrick, Potter & Hoar, 1991). Insights into g_{app} can be gained by examining the changes in the concentration of Ca^{2+} required to elicit 50% of maximal force or ATPase activity ($[Ca^{2+}]_{50}$) of the force - free Ca^{2+} and ATPase - free Ca^{2+} relationships. For example, if g_{app} contributes to XB force regulation it would be expected that Ca^{2+} sensitivity would differ between ATPase and force such that A/F would be large at intermediate levels of free Ca^{2+} and small at maximal levels.

The overall objective of this investigation was to probe the potential role of g_{app} in the regulation of force output at the level of the XB. Accordingly the specific aims of the project are:

1. To determine whether g_{app} is sensitive across a physiological range of Ca^{2+}
2. To determine if g_{app} can be altered by biochemical manipulations (i.e., decreased [MgATP]) which are predicted to affect g_{app}.
3. To determine whether differences in g_{app} exist between fibers with known differences in XB cycling kinetics (e.g., fast and slow)
4. To determine the sensitivity of fast and slow fibers to reduced [MgATP] which is predicted to affect g_{app}.

Research Hypothesis

Specifically this investigation will test the following null hypotheses:

H_o There will be no difference between the force and ATPase free Ca^{2+} relationship across a physiological range of Ca^{2+}.

H_o There will be no difference in $[Ca^{2+}]_{50}$ between force and ATPase at 2.0, 1.0, 0.5, and 0.25 mM MgATP.

H_o There will be no difference in $[Ca^{2+}]_{50}$ of force and ATPase between muscles with differing contractile characteristics (i.e., fast and slow fiber types).

H_o There will be no difference in $[Ca^{2+}]_{50}$ of the force and ATPase at 2.0 and 0.5 mM MgATP between fast and slow fiber types.

Delimitations

The following delimitations were imposed on the study by the investigator:

1. The investigation was delimited to skeletal muscle fibers obtained from frog semitendinosus muscle, mouse extensor digitorum longus (EDL) muscle, and rat soleus and EDL muscle.
2. The measurement conditions were delimited to a imidazole propionate buffered experimental solution maintained at 20°C, pH 7.0, and .18 M ionic strength.
3. The results were delimited to the following parameters which describe the force and ATPase-free Ca^{2+} relationship; $[Ca^{2+}]_{50}$, n (the Hill slope of the relationship), F_{max} (maximal Ca^{2+} activated force), and A_{max} (maximal ATPase activity).

Limitations

The following limitations of the study were recognized by the investigator:

1. Due to the specific experimental temperature, results are limited to data collected at similar temperatures.
2. Due to methodological considerations, sarcomere length was not controlled during the investigation.

Basic Assumptions

The following assumptions were made prior to the start of the investigation:

1. All experimental animals possessed normal anatomy and were free of disease.

2. The incubation solution adequately reflects the intracellular milieu of frog and rat skeletal muscle.

3. Changes in NADH accurately reflect ATP utilization.

Definitions and Symbols

ATPase	Myosin ATPase activity
A/F	ATPase and force ratio (estimate of g_{app})
Ca^{2+}	Free calcium ion
$[Ca^{2+}]_{50}$	Calcium concentration at which force is 50% of F_{max}
$[Ca^{2+}]_i$	Intracellular calcium
F_{max}	Maximal calcium activated force
A_{max}	Maximal calcium activated ATPase activity
f_{app}	The apparent rate constant for the transition of the weak binding cross-bridges to the strong binding state.
g_{app}	The apparent rate constant for the transition of the strong binding crossbridges into the weak binding state.
SB	The strong binding state of actin and myosin associated with force generation
WB	The weak binding state of actin and myosin associated with no force generation
XB	Actin - Myosin cross-bridge

F_{av}	Average force per cross-bridge
pCa	Expression of free Ca^{2+} in units of -log [Ca^{2+}]
N	Slope of the ATPase of force free Ca^{2+} relationship
n	Number of cross-bridges per half sarcomere
k_{tr}	Rate of tension redevelopment after a fiber is quickly shortened and restretched to original length ($k_{tr} = f_{app} + g_{app}$)
b	Number of half sarcomeres

REVIEW OF THE LITERATURE

> "All living cells are really chemical machines, and we can never understand them properly until we know the nature of the chemical processes which go on inside them. It might have been imagined that by looking closely at a muscle-fiber under a microscope we should have been able to find out something about the nature of its machinery. For generations people have examined muscle by such means but with little result. Various things have been seen in muscle, various theories have been invented relating the structures observed to the behavior of the machine. ...The truth would seem to be that the real machinery of the muscle is far to small to see; it is, so to speak, of molecular dimensions. ...As it is, the properties of a contracting muscle seem to depend upon obscure chemical properties of unknown chemical substances, which tend, for unknown reasons, when we stimulate the muscle, to fall into some new orderly but unknown arrangement. One thing, however, would seem certain, namely, that the machine is chemical in nature." Living Machinery *A.V. Hill. 1927*

Introduction

Over the past century much progress has been made in understanding the skeletal muscle contraction process. Investigations in the disciplines of physiology, biochemistry and biophysics have contributed to the current understanding of the cellular regulation of muscle contraction. This review provides an overview of the structure and function of the contractile apparatus and discusses some of the theories which have contributed to the current understanding of the contraction process.

Overview of Contractile Apparatus Structure

The structure of the contractile apparatus has been described by others (Shepard,

1982; Berne and Levy, 1988), thus a brief overview will be presented here. Examination of gross muscle structure reveals an striation pattern which is the result of the repeating pattern of the structural components of the myofibrils within a muscle cell. Within a muscle cell, bundles of myofibrils are arranged along the long axis and in register along the transverse axis of the cell. This striation pattern arises from two sets of myofilaments which make up the myofibrils. The dark striations are a region containing a lattice of thick filaments. A second lattice contains the thin filaments which are attached to a transverse structure called the Z line. The thin filaments extend from two adjacent Z lines to interdigitate with the thick filament lattice. The thick and thin filaments bounded by two Z lines form the functional contractile unit of the muscle cell termed the sarcomere. Within the sarcomere thick and thin filaments interdigitate and slide past one another to allow fiber shortening.

The contractile filaments are held in place by several cytoskeletal proteins (Berne and Levy, 1988). Titin is a large elastic protein which links myosin filaments to adjacent Z lines. Nebulin is a rigid protein which attaches the thin filaments to the Z lines, and desmin is also a rigid protein which connects the adjacent Z lines of adjacent myofibrils. These cytoskeletal proteins provide the structural support which enables the sarcomeres to remain organized in horizontal and transverse register during shortening contractions.

Thin filaments are formed from two major proteins, actin and tropomyosin. The thin filament backbone is composed of a series of F-actin filaments. F-actin is composed of globular actin (g-actin) monomers arranged in a α-helical two stranded filament. Along

both grooves formed by the α-helical arrangement of the actin filaments lie two tropomyosin (TM) molecules. Each TM molecule is composed of two TM dimers and spans seven g-actin monomers. At the end of the tropomyosin molecules clusters of three troponin polypeptide subunits are bound: Troponin -T binds the troponin molecule; Troponin-C has binding sites for Ca^{2+} ions; and Troponin-I inhibits G-actin from binding to the thick myofilament (Payne and Rudnick, 1989). This troponin complex comprises the Ca^{2+} sensitive regulatory mechanism of skeletal muscle.

The thick filament is composed of myosin. The myosin molecule can be subdivided into its functional domains by proteolytic cleavage with trypsin or papain. The cleavage points coincide with sites at which the α-helical structure is structurally altered, i.e., sites that allow flexion or movement. With these enzymes, myosin can be cleaved into a long (LMM) and a short (HMM-S2) rod segment and two globular heads (HMM-S1). Each 'head' contains the myosin-ATPase enzyme and an actin binding site. The HMM can be further subdivided into two subfragments with S-1 containing the globular head region and S-2 containing the flexible neck region which joins the HMM to the LMM region.

In three dimensional orientation each myosin is in an tail-to-tail association with another myosin molecule. This bipolar myosin complex associates with many other myosin complex resulting in a thick filament of myosin with many HMM processes on each end and a central zone free of HMM processes. This thick filament is surrounded by six thin filaments in a cylindrical relationship with the S-2 filament and myosin heads spanning the distance with bonds to actin.

The myosin molecule is formed by the association of six different polypeptides. These peptides can be dissociated by denaturation and separated into one pair of heavy chains and a two pairs of light chains. In the intact thick filament the pair of heavy chains form the α-helical rod portion with the two globular heads, one formed from each heavy chain. Muscle can genetically express several types of heavy chains. In fact, it appears that muscle adaptation to altered demand is, at least in part, linked to differing heavy chain isoforms (Staron and Johnson, 1993). These isoforms have been traditionally been identified by the density of histochemical staining based on pH stability but functionally they are grouped by differing rates of ATP hydrolysis, i.e., slow or fast ATP hydrolysis. In the human, the predominant heavy chain isoforms are the type I slow isoform and the type IIa and IIb fast heavy chain isoforms. Other species such as the rat (Bottinelli, Canepari, Reggiani and Stienen, 1994) express intermediate heavy chain isoforms such as type IIx which is intermediate to the IIa and IIb in ATP hydrolysis rate.

Myosin light chains are associated with each myosin head and seem to play a regulatory role in actin and myosin interactions (Staron & Johnson, 1993). Each myosin is associated with a pair of two identical phosphorylatable (P) light chains and a pair of either two identical or non-identical alkali light chains. These light chains associate with the myosin head with one polypeptide from each of the light chain pairs associating with each individual myosin head. Much like the heavy chains, both alkali and P light chains exist in fast and slow isoforms

Early Theories of Muscle Contraction

Theories on the biology of movement can be found as early as the third century B.C. in the writings of the Hippocratic collection on medicine and its philosophy. The Greek scholars and philosophers of this era believed that bones provided a structure for support, the skin and flesh (muscle) provided substance and arrangement to the body, and blood vessels supplied air to the nerves for the power of movement (Machina Carnis, 1971). The basis for this belief was the theory of *pneuma* in which "breaths" or "air" traveled with the blood to the nerves in order provide a pneumatic mechanism for movement. In fact this theory of *pneuma* encompassed so much of the understanding of biology that even sleep was ascribed to "air" settling in the chest and abdomen since sleep was proceeded by yawning.

The first widely accepted modern theory of muscle contraction was proposed by A.F. Huxley in 1957. In the *Sliding Filament Theory*, Huxley (1957) proposed that the sliding of actin past myosin was driven by actin-myosin XB formation and powered by ATP hydrolysis. These ideas were based on knowledge of both myofibrillar structure and actinomyosin ATPase activity and the idea that the interaction of actin and myosin occurred in a cyclic "oar-like" fashion.

Within the muscle cell, force production is closely matched to the level of $[Ca^{2+}]_i$. At the cellular level, force can be described by the sigmoidal relationship between free Ca^{2+} and force production (Figure 1). In the resting cell most Ca^{2+} is sequestered in the sarcoplasmic reticulum (SR) leaving the myoplasmic concentration around 50 nM. At this

level of Ca^{2+} no detectable force is generated by the contractile apparatus. Increasing levels of $[Ca^{2+}]_i$ elicit increased force output until maximal tension is realized at 5-10 μM Ca^{2+}. Relaxation of the system occurs when Ca^{2+} is re-sequestered into the SR (Berne and Levy, 1988).

In 1971, Huxley and Simmons (1971) proposed an experimental model to explain the kinetics of the XB cycle as it was then understood. This model consisted of two states, a non-force generating state which represented unbound actin and myosin, and a force generating state which was realized when actin and myosin was bound. Transition between these two states was described by a rate constant which encompassed transition from the non-force to force generating state and a rate constant for the return to the non-force generating state. This model reasoned that contractile force increased with increasing levels of Ca^{2+} by causing an increase in the fraction of crossbridges in the force generating state. The opposite circumstance of decreasing Ca^{2+} returned the crossbridges to the non-force generating state causing relaxation. In short, Huxley believe that force was regulated by a Ca^{2+} sensitive XB recruitment.

During the mid 1970's, studies utilizing X-ray diffraction (Parry and Squire, 1973) and electron microscopy (Gillis and O'Brien, 1976; Eaton, 1976) lead to the steric blocking model as a proposed mechanism to describe XB recruitment and force generation in striated muscle. In this model, at low Ca^{2+} concentration, the tropomyosin molecule is positioned on the peripheral edge of the F-Actin groove. In this position, tropomyosin blocked the myosin binding site thus preventing the binding of the myosin head to the actin

filament. Increasing levels of intracellular Ca^{2+} resulted in the binding of Ca^{2+} to the low affinity binding sites on Tn-C. This binding caused a physical rotation of the tropomyosin molecule into the thin filament groove uncovering the myosin binding site on actin thus allowing actin and myosin to bind. Actin and myosin binding was then thought to initiate ATP hydrolysis and movement of the myosin head thus allowing the XBs to slide past one another. Thus, in this model, Ca^{2+} regulates force by allowing the myosin greater access to actin and increased XB recruitment.

Since the 1970's a the steric blocking model has been the most widely described model in textbooks. While the steric blocking model fit well with the data describing the structural mechanisms of muscle contraction in the 1970's, specific details regarding the XB cycle were still unknown. In order to further understand the XB cycle, effort was focused on the mechanism by which ATP hydrolysis was linked to XB attachment, subsequent movement of the myosin head, and XB detachment.

Recently, Schutt and Lindberg (1992) have proposed an alternative theory of muscle contraction. These authors suggest that actin is the primary generator of force during contraction. In this model, force develops as actin is transformed from a flat ribbon like orientation to a helical orientation. Specifically, this model proposes that an actin filament attaches on one end to tropomyosin and on the other end to a myosin head. As actin transforms from a ribbon to a helical structure, actin pulls tropomyosin while being anchored to the thick filaments by myosin resulting in fiber shortening. Despite this model accounting for many of the features of the contraction process this theory is not widely

accepted as the mechanism for muscle contraction.

The Cross-bridge Cycle: Biochemical studies of the Actin-Myosin ATPase cycle

Early models attempting to explain the biochemical mechanisms of the XB cycle were based on the interaction of actin and myosin fragments in solution. Eisenberg & Moos (1968) examined the interaction of myosin subfragment S-1 and actin in solution and determined that: 1) ATP binding to myosin S-1 greatly weakened the S-1 bond to actin, and 2) S-1 binding to actin substantially increases myosin ATPase activity. Based on these findings Eisenberg & Moos developed a kinetic model for the XB-ATPase relationship which predicted that actin (A) and myosin (M) oscillate between A·M and A·M·ATP without myosin dissociating from actin. While this model accounted for the ATPase activity of bound actin and myosin, it failed to address a mechanism for myosin detachment from actin following the ATP hydrolysis.

Lymn and Taylor (1971) further expanded on the work of Eisenberg & Moos (1968) based on two additional pieces of evidence. First, it was discovered that in the absence of actin, myosin hydrolyses ATP to ADP and inorganic phosphate (Pi) much more rapidly than ADP and Pi release into solution. Second, ATP was reported to dissociate the actin-myosin XB bond into M·ATP+A even faster than the hydrolysis of ATP to ADP and Pi. With these pieces of evidence, Lymn and Taylor (1971) proposed a model in which ATP dissociated A·M into M·ATP + A and the resultant hydrolysis of ATP to ADP and Pi only occurred on the dissociated myosin. When myosin was bound to actin, ATP

hydrolysis did not occur.

Stein et al. (1979) reported data which further refined the understanding of the XB cycle. In opposition to the Lymn and Taylor (1971) model which suggested that ATP binding to myosin irreversibly dissociated actin and myosin, Stein et al. (1979) reported 1) M·ATP binds to actin to an equivalent degree as M·ADP·Pi. and 2) myosin with either ATP or ADP·Pi bound is in rapid equilibrium with actin. Stein et al.(1979) also reasoned that myosin is not required to dissociate from actin in the XB cycle and ATP is not hydrolyzed only when actin and myosin are unbound. With this data Stein et al.(1979) (Figure 3) proposed a kinetic model for actin and myosin interaction in which myosin undergoes a transition between a weak binding conformation and a strong binding conformation with each XB cycle being marked by hydrolysis of ATP.

Other models have been proposed which characterize the XB cycle (Huxley and Simmons, 1971; Bagshaw, Eccleston and Eckstein, 1974). While each model offers slight variations in biochemical steps and kinetic scheme, all of the models share some common features. All agree on three concepts: first, there are two categories of XB configuration. The WB is a category of weak binding configurations which do not contribute to force generation. These weak binding states are described by myosin binding in rapid equilibrium and with low affinity to the actin filament. This interaction occurs without Ca^{2+} present and is characterized by ATP or its hydrolysis products (ATP and Pi) bound to the myosin head. The SB is a group of strong binding states distinguished by a Ca^{2+} dependent actin-myosin interaction, a several fold increase in myosin's affinity for actin, and actin and

myosin binding with a slowed rate of actin-myosin dissociation. Second, there is a rate limiting step in the XB cycle which controls the transition between the weak binding XBs and strong binding XBs. Finally, a possible regulatory step in the XB cycle is the rate constants between the two XB states.

Recently Higuchi and Goldman (1995) suggested that more than one XB cycle occurs with a single ATP hydrolyzed based on the distance of fiber shortening per amount of ATP hydrolyzed. While those data could have an impact on the current understanding of the XB cycle, the results of that investigation have yet to be verified by others.

For the purposes of this literature review, the XB cycle (Figure 3) will be summarized in the six state model of Stein et al. (1979). This remains a widely accepted model of the biochemical steps of the XB cycle. The first state is a group of weak binding configurations which do not contribute to force generation. In this state myosin binds rapidly and with low affinity to the actin filament. This state is characterized by ATP or its hydrolysis products (ATP and Pi) bound to the myosin head. Ca^{2+} binding to troponin-C causes all the troponin subunits to bind less tightly to actin initiating a slight conformational change in the troponin complex. Instead of an "uncovering of a binding site' as previously thought, three events take place: the affinity of actin to myosin is increased several magnitudes, the kinetics of ATP hydrolysis is increased, and Pi is released from the myosin head.

Following the release of Pi, the cross-bridges enter into a series of configurations that make up the strong binding state. In this state, energy release is utilized to shift the

myosin head from a 90° configuration relative to actin to a 45° configuration. This action causes the myosin head to "contract" toward the center of the thick filament. The XB movement is the mechanism by which the actin and myosin filament slide past one another as described in the *Sliding Filament Theory.*

During the strongly bound state ADP is released forming a XB rigor bond which remains until a new ATP is bound to the myosin head. The binding of the ATP molecule drastically reduces the affinity of myosin and actin, allowing the XB to return to a weakly bound "relaxed" state. While an ATP molecule is needed for the transition back to the weakly bound state it does not need to be hydrolyzed to do so. This cycle is repeated as long as Ca^{2+} is present to bind to Troponin-C and as long as ATP is present.

While this model describes the steps of the XB cycle, it does not predict how Ca^{2+} influences force production. Force at the level of the XB is dependent on the number of XBs, force produced per XB and the rates at which the XBs cycle into and out of the force generating state.

Cross-bridge Cycling Kinetics

Based on Huxley's model (1957), the XB cycle is a Ca^{2+} sensitive system in which XBs cycle between a non-force generating (NF) and force generating (F) state while being powered by ATP hydrolysis. In this model force is produced by increasing the percentage of XBs in the force generating state. Relaxation then occurs when a critical proportion of XBs are shifted back to the non-force generating state. Based on biochemical and

structural data of the contractile protein interactions, Brenner (1986,1988) and Brenner and Eisenberg (1987) proposed a kinetic model to describe the XB cycle (Figure 4). Similar to the Huxley model a two state model was developed with XBs cycling between a group of strongly bound (SB), and a group of weakly bound (WB) states (SB is force generating and WB is non-force generating). Unlike the Huxley model which used 'f' and 'g' to denote the transition between the XB states, Brenner utilizes 'f_{app}' and 'g_{app}' to define the apparent rate constants which encompass several biochemical steps in the transition between the states. In Brenner's scheme f_{app} represents the sum of the rate constants which determine the XBs move from the WB to the SB state while g_{app} represents the return to the WB state.

Brenner (1988) developed a series of equations which he used to examine how the XB cycle influences force generation. These equations have lead to studies designed to understand how Ca^{2+} influences force generation at the XB.

In Brenner's model (1988), the fraction of cycling myosin cross bridges (F_s) in the force generating state at any one time is defined as

$$F_s = f_{app}/(f_{app}+g_{app}) \qquad [1]$$

With this equation the isometric force (F) and fiber stiffness (S) of a half sarcomere can be calculated by

$$F = n \bullet F_{av} \bullet [f_{app}/(f_{app}+g_{app})] \qquad [2]$$

$$S = n \bullet S_{av} \bullet [f_{app}/(f_{app}+g_{app})] \qquad [3]$$

Where n is the number of XBs per half sarcomere, F_{av} is the average force per cross bridge head, S_{av} is the average stiffness per cross-bridge.

Isometric force of a fiber can be calculated by incorporating the volume terms of myosin concentration ([M]), fiber cross sectional area, (A), and length of a half sarcomere ($L_{1/2s}$)

$$F = F_{av} \cdot [M] \cdot A \cdot L_{1/2s} \cdot [f_{app}/(f_{app}+g_{app})] \quad [4]$$

Assuming that myosin hydrolyzes 1 ATP per head per XB cycle (Lymn & Taylor, 1971), ATPase activity of a sarcomere during an isometric contraction can be expressed as

$$ATPase = n \bullet b \bullet g_{app} \bullet [f_{app}/(f_{app}+g_{app})] \quad [5]$$

with n representing the number of XBs per half sarcomere and b being the number of half sarcomeres in a fiber.

ATPase of a fiber can be calculated by incorporating volume terms of myosin concentration ([M]), number of half sarcomeres (b), fiber cross sectional area (A), and length of a half sarcomere ($L_{1/2s}$).

$$A = [M] \cdot b \cdot A \cdot L_{1/2s} \cdot g_{app} \cdot [f_{app}/(f_{app}+g_{app})] \quad [6]$$

Dividing ATPase by the force:

$$ATPase/F = g_{app} \bullet (b/F_{av}) \quad [7]$$

In this model, XB cycling rate is defined as the sum of the rate constants governing the transition between WB and SB and vice versa. (i.e., $f_{app} + g_{app}$). At a given level of

activation it is possible to determine the velocity of this kinetic cycle by measuring the rate constant of tension redevelopment after a Ca^{2+} activated fiber is quickly shortened and restretched (k_{tr}). In this technique an activated fiber is rapidly shortened to allow the XBs to cycle at maximal velocity for 20-50 msec. The fiber is then rapidly restretched to original length which effectively dissociates all actin and myosin XBs. The rate at which the force returns to the original level after the restretch represents the maximal cycling rate of the XBs (i.e., k_{tr}). This estimation is independent of the number of cycling crossbridges and is defined as :

$$k_{tr} = f_{app} + g_{app} \quad [8]$$

Given that F_{av} is constant under normal conditions (Brenner, 1988) and the # of half sarcomeres (b) does not change within experimental conditions, equation [7] can be reduced to

$$g_{app} \propto \text{ATPase/F} \quad [9]$$

Thus, the simultaneous measurement of force output and myosin ATPase activity of a muscle fiber allows an estimate g_{app}.

With a value for k_{tr} [8] it is possible to reduce equation [2] to equation [10]. Since n and F_{av} are accepted as being constant (Brenner, 1988) f_{app} can be estimated by equation [11].

$$F \cdot k_{tr} = n \cdot F_{av} \cdot f_{app} \quad [10]$$

$$f_{app} = F \cdot k_{tr} \quad [11]$$

Regulation of Cross bridge Force: The Cross-bridge Kinetic cycle

In order to determine the contribution of the apparent rate constants to Ca^{2+} sensitive increases in force, measurements of isometric force, fiber stiffness, myosin ATPase, and tension redevelopment after quick release and restretch can be utilized to obtain estimates of f_{app} and g_{app}. With these measurements Brenner (1986 & 1988) first demonstrated that k_{tr} was sensitive to increases in Ca^{2+} but was not affected by increasing isotonic load at different levels of Ca^{2+} activation. These data suggest that the maximal XB cycling rate is dependent on Ca^{2+} activation but is not dependent on force production. It was therefore concluded that k_{tr} represents the approach of the cycling XBs to the isometric steady state and that Ca^{2+} acts to alter the XB cycling kinetics (f_{app}+g_{app}) in regulating force production. Other investigators have now confirmed that k_{tr} is Ca^{2+} sensitive at several experimental temperatures (Metzger et al.1990, Metzger and Moss 1990, Chase, Martyn and Hannon 1994).

Isometric force and fiber stiffness have been used to estimate the amount of force contributed by each cross-bridge. While force is the determined by the amount of force produced by the cycling XBs, stiffness is a estimate of the number of bound crossbridges in the force generating state. When stiffness is plotted against force a linear relationship results suggesting that the number of XBs in the SB state increases in proportion to

increasing force (Brenner, 1986).

If the ratio of stiffness (S) to force (F) is investigated across activating levels of Ca^{2+} the force produced per cross-bridge can be deduced. Brenner (1988) has shown that S_{av}/F_{av} is constant across physiological levels of Ca^{2+}. Since it is highly unlikely that changes in F_{av} are matched by identical changes in S_{av} (thus keeping the ratio of S_{av}/F_{av} constant) it is accepted that these parameters remain constant through all levels of Ca^{2+} activation. These data support the idea that S_{av} and F_{av} are not Ca^{2+} sensitive. If control of crossbridge force output is not due to an increase in F_{av} or an increase in the population of cycling crossbridges, the rate constants governing the kinetic cycle (f_{app} & g_{app}) must regulate XB force.

Brenner (1988) utilized the ratio of ATPase to force (A/F) (equation [9]) in skinned rabbit psoas fibers to determine the role of g_{app} in the XB cycle. In this investigation A/F remained virtually unchanged across levels of Ca^{2+} activation. With A/F being a estimate for g_{app}, Brenner (1986 & 1988) concluded that g_{app} is insensitive across a physiological range of Ca^{2+} . With the findings that g_{app} does not change with Ca^{2+} activation while k_{tr} does, Brenner (1986 & 1988) concluded that f_{app} must change with Ca^{2+} activation. These data confirmed the findings of Pemrick (1980) who reported that, in solution, the Ca^{2+} sensitivity of the myosin S-1 ATPase in the presence of actin was unchanged with myosin light chain phosphorylation. Since myosin light chain phosphorylation is known to increase XB cycling and the calcium sensitivity of the ATPase did not change with phosphorylation, it was concluded that g_{app} did not change.

This conclusion supports the idea that g_{app} is not Ca^{2+}sensitive, thus leaving f_{app} as the primary regulator of the XB kinetic cycle.

Brenner (1988) ultimately showed a positive sigmoidal relationship between Ca^{2+} concentration and f_{app}. In fact increases in f_{app} were seen at all levels of Ca^{2+} activated force with f_{app} increasing in an exponential manner above 40% isometric force. In brief, reports by Brenner (1986 & 1988) suggest that: first, k_tr represents the isometric XB turnover kinetics which are defined as $f_{app} + g_{app}$. Second, the number of cycling XBs remain relatively constant across levels of activation. Third, g_{app} remains constant with Ca^{2+} activation. Based on these findings, Brenner concludes that f_{app} regulates the XB cycle while g_{app} remains unchanged with Ca^{2+} activation.

While data was mounting in favor of f_{app} as the primary regulator of the XB cycle, Kerrick et al.(1990), made simultaneous measurements of ATPase and force in skinned rabbit psoas fibers in order to determine the Ca^{2+} sensitivity of the estimate of g_{app}. As mentioned previously g_{app} can be estimated by the ATPase to force ratio as described in equation [9]. In opposition to the aforementioned investigations, Kerrick et al.(1990) reported that in rabbit psoas muscle at 20°C, the force-free Ca^{2+} relationship was shifted to the right ($P<0.05$) of the ATPase-free Ca^{2+} relationship. In fact the pCa_{50} (- log $[Ca^{2+}]_{50}$) for force and ATPase were 5.68 and 5.40 respectively. This separation in the ATPase and force-free Ca^{2+} relationship resulted in estimates of g_{app} (i.e. A/F ratio, Equation [7]) exhibiting a five-fold decrease across submaximal levels of Ca^{2+} activation. Since the number of cycling XBs remains constant with increasing Ca^{2+}activation and the number of

half sarcomeres also remains constant, any changes in the A/F ratio are hypothesized to be due to g_{app}. These data suggesting that estimates for g_{app} are Ca^{2+} sensitive. These results are in opposition to data reported by Brenner (1986 & 1988) in rabbit psoas at 5°C in which the A/F ratio (g_{app}) remained virtually unchanged with increasing activation. Taken together, the data from Brenner (1986&1988) and Kerrick et al. (1990) suggest that f_{app} and g_{app} both play a role in regulating XB force.

Using some simplifying assumptions it is possible to demonstrate the influence of f_{app} and g_{app} on force and ATPase activity. Assuming that n and F_{av} from equation [2] are constants (Brenner, 1988), force can be defined as $F = f_{app} / f_{app} + g_{app}$. While also assuming that n and b in equation [5] are constants (Brenner, 1988), ATPase can be summarized by $A = g_{app} \cdot f_{app} / f_{app} + g_{app}$. Substituting in known values for f_{app} and g_{app} (Brenner, 1986) it is possible to examine the result of altering these apparent rate constants on force output and myosin ATPase activity. Initially setting f_{app} at $24s^{-1}$ and g_{app} at $2.8s^{-1}$, F = .90 and A = 2.51 (arbitrary units), the effect of reducing g_{app} by half to $1.4s^{-1}$ causes a slight increase in F to .94 but causes a decrease in A to 1.32 (arbitrary units) which is almost half of its original value. Alternatively, reducing f_{app} by half to $12s^{-1}$ while holding g_{app} constant at $2.8s^{-1}$, causes both a reduction in F to .81 and a reduction in A to 2.27 (arbitrary units). Therefore it appears that while decreases in f_{app} depress force and ATPase activity, reductions in g_{app} increase force while reducing ATPase activity by nearly a half. Therefore, it is evident that alterations in the values for the apparent rate constants can affect force output and energy consumption of the XBs.

The Weak Binding State

Identification of the WB state has lead to much debate as to its importance in force regulation at the XB. Initial observations of myosin (HMM & S-1) binding to actin in solution showed substantially stronger binding in the presence of ADP when compared to ATP. This resulted in the identification of the WB state (Chalovich and Eisenberg, 1982). Since the force associated with the WB state is weak and the amount of actual WB interactions was thought to be small, it was initially thought that the WB state was a relatively unimportant intermediate step in the XB cycle.

Despite the results from actin-myosin interactions in solution, it was felt that the WB XB could play a significant role in the intact fiber even though the binding was weak. In the intact fiber, the myofilaments are organized as a lattice structure which provides a much greater effective actin to myosin concentration (i.e., greater possibility of XB interaction) than that seen in solution (Brenner, 1986). To determine the contribution of WB XBs in muscle fibers, Brenner, Schoenberg, Chalovich and Greene (1982) made rapid stiffness measurements in relaxed skinned fibers. In this investigation, these authors reported that the number of WB XBs in relaxed fibers can be as great as 50% of the number of WB XBs seen in rigor conditions. These data suggest that the WB state can play a role in regulating fiber stiffness in a fiber that is producing no detectible force.

Caldesmon, a smooth muscle protein, has been shown to selectively bind to actin and competitively inhibit the binding of the WB XBs without affecting the binding of the

SB XBs. The binding constant of caldesmon to actin has been shown to be similar to the binding constant for SB XBs while it is much greater than the binding constant for the WB XBs (Velaz, Ingraham and Chalovich, 1990). This protein has been used to probe the importance of the WB XBs in force regulation. Brenner (1991) has reported that while stiffness is decreased by 20% in activated fibers with caldesmon, no change in stiffness is seen in fibers in rigor following incorporation of caldesmon. Since in rigor conditions, the XBs remain in the SB state, these data suggest that caldesmon acts specifically on the WB state.

Chalovich, Yu and Brenner (1991) used caldesmon to probe the function of the WB XBs at low temperature (5°C) and low ionic strength (.02 M) conditions. At low ionic conditions the myofiliment lattice structure is separated such that the thin and thick filament distance is increased. This separation results in a decrease in the effect of the WB XBs without significantly effecting force generation. As concentrations of caldesmon were increased, there were parallel decreases in both stiffness in relaxed fibers and force in activated fibers. Since conditions were such that only the WB XBs were inhibited, it was concluded that the inhibition of the WB caused the decline in force and stiffness. Therefore XB transition through the WB state seems to be essential for XB force production. These conclusions have also been supported by a recent report from Kraft, Chalovich, Yu and Brenner (1995) who has demonstrated that active force and fiber stiffness decreased with caldesmon at near physiologic temperatures (30°C) and physiological ionic strength (0.17 M).

Fast vs Slow Muscle

Much data are available showing differences in the contractile characteristics between fast and slow muscles. Fast muscle is known to reach maximal tension faster and relax faster when compared to slow muscle. Single fiber investigations have also demonstrated that while maximal isometric force (F_{max}) (normalized by cross sectional area) is not different between fiber types, slope of the curve (N), $[Ca^{2+}]_{50}$, and maximal myosin ATPase activity (A_{max}), are all increased in fast fibers.

The mechanisms which underlie the difference in Ca^{2+} sensitivity between fiber types have not been identified. Metzger and Moss (1990) proposed that XB cycling differences between fast and slow fibers might play a role in the differing Ca^{2+} sensitivity between the two fiber types. Metzger and Moss (1990) utilized measurements of k_{tr} and showed that at maximal activation, k_{tr} exhibited a four fold increase in (fast) psoas fibers when compared to (slow) soleus fibers of the rabbit. As mentioned previously, k_{tr} represents the maximal XB cycling rate and is independent of n and F_{av}. Thus, k_{tr} can be defined as the sum of the two apparent rate constants f_{app} and g_{app}. While it was apparent that XB cycling differed between fast and slow muscle, it is not known whether f_{app} or g_{app} or both contribute to the differences in XB cycling between fast and slow fibers.

Modulation of XB Force

Experiments which involve the manipulation or removal/replacement of regulatory

proteins have provided evidence that regulatory proteins act to modulate XB force (Moss, 1992). These investigations have provided valuable information on the regulatory mechanisms of the XB cycle.

As mentioned previously, Metzger (1990) found that the phosphorylation of myosin light chain two (LC2) altered the k_{tr} in skinned fibers. Further examination of LC2's role in modulating XB function was performed by Hoffman, Metzger, Greaser, and Moss, (1990). In this investigation tension, stiffness and k_{tr} were examined at various levels of Ca^{2+} activation with varying degrees of LC2 extraction. Extraction of 20-40% of LC2 resulted in increased tension at submaximal activation but had no effect on maximal activation. The drop in submaximal tension resulted in a leftward shift of the force free-Ca^{2+} relationship. Stiffness was increased in proportion to the increased submaximal tension while maximal stiffness was unchanged. Also, velocity of shortening decreased with LC2 extraction. Together, the results by Metzger et al. (1990) and Hoffman et al (1990) suggest that LC2 regulates contraction by modulating the number of XBs formed (changes in stiffness) and by modulating the velocity of shortening (increases in k_{tr} with phosphorylation; decreases in k_{tr} with LC2 extraction). The effect of LC2 phosphorylation on the apparent rate constants was investigated by Sweeny and Stull (1990). These authors reported that in rabbit fast skeletal muscle, increases in f_{app} with Ca^{2+} activation were further increased with LC2 phosphorylation while A/F (g_{app}) remained constant. These data suggest that the increases in k_{tr} with phosphorylation are solely due to increases in f_{app}.

Force regulation at the XB is a highly cooperative process in which small increases in Ca^{2+} elicit large increases in tension above the threshold for Ca^{2+} activation of force. Initiation and regulation of XB force under physiologic conditions requires that Ca^{2+} be bound to the low affinity binding sites on Tn-C. To emphasize this point, partial extraction of Tn-C from skeletal muscle fibers showed reduced F_{max} and reduced Ca^{2+} sensitivity (Brandt, Diamond, and Schachat, 1984). Also Brandt, Diamond, Rutchik, and Schachat (1987) reported that extraction of as little 5% of total Tn-C significantly altered the force free-Ca^{2+} relationship. The contribution of the type of Tn-C in the determination of the force free-Ca^{2+} was investigated by Moss (1992) who extracted native Tn-C from skinned skeletal muscle fibers and subsequently replaced them with the cardiac Tn-C. While F_{max} was reduced by less than 10%, the Ca^{2+} sensitivity was increased with the slope of the force free-Ca^{2+} relationship showing a slight depression.

Evidence for cooperative activity at the level of the XB was reported by Bremel and Weber (1972) who demonstrated that in solution, Ca^{2+} affinity to the Tn-C was increased when the S-1 fragment was bound to actin in the absence of MgATP. Similar findings have been reported in skinned fibers with the force-free Ca^{2+} relationship becoming more sensitive with decreased [MgATP] (Kerrick et al 1990, Brenner 1986).

Summary

Significant progress has been made in elucidating the steps involved in the production of whole muscle force. Despite this, the specific mechanisms of force regulation at the level

at the XB, and mechanisms which underlie the differences in contractile characteristics between fast and slow muscle remain unclear.

It is evident that Ca^{2+}regulation of XB force production is modulated by cross-bridge cycling kinetics, i.e., apparent rate constants (f_{app} and g_{app}) which represent the biochemical steps in the transition between the weakly bound (non-force generating) and the strongly bound (force generating) XB states. It has been demonstrated that f_{app} is Ca^{2+} sensitive and suggested that f_{app} is most likely the primary regulator of force production. However, even though alterations in XB force and XB cycling can be accounted for by altering f_{app}, g_{app}, or both, the role of g_{app} remains unclear.

RESEARCH DESIGN AND METHODS

Introduction

The experimental technique employed in this investigation is a skinned fiber preparation. With this technique, functional measurements (i.e., isometric force and energy consumption) of contractile apparatus function are made on single cut pieces (~ 70μm diameter, 1-2mm length) of skeletal muscle fiber. The unique feature of this procedure is the ability to precisely monitor functional performance of the contractile apparatus with the ability to selectively control the physiological environment (bathing solution) around the contractile apparatus.

While this investigation employs modern equipment and methods to determine the functional characteristics of the skinned fibers, it is of interest to note that the skinned fiber technique has been utilized since Szent-Györgyi (1949) developed and reported use of the a glycerinated skinned single muscle fiber preparation from the rabbit. Early investigations employed rather unsophisticated measurements of contraction and relaxation with this technique but made large strides in understanding the effects of ATP and other ions on the contraction and relaxation of muscle fibers. Since 1949, countless investigations have examined the function of the contractile apparatus using this technique in the pursuit of understanding the mechanism and regulation of muscle contraction (Machina Carnis, 1971).

Experimental Designs

Specific Aim 1

The first aim of this investigation was to determine if g_{app} plays a role in force regulation by the contractile apparatus. If g_{app} is important in the XB cycle it would be expected that at least two conditions would be satisfied. First, g_{app} must exhibit calcium sensitivity, i.e., it should vary as a function of free-Ca^{2+}. Second, biochemical manipulations which are predicted to alter the XB cycle should alter g_{app}, i.e., altering the kinetics of the XB cycle should affect both the magnitude and Ca^{2+} sensitivity of g_{app}. Accordingly, the following experiments were performed.

Experiment 1. The purpose of the first experiment was to determine if g_{app} changes across a physiological range of calcium concentration. Single muscle fibers were dissected from whole frog semitendinosus muscles and chemically skinned. Isometric force and myosin ATPase were measured simultaneously across a physiological range of Ca^{2+}. The magnitude and Ca^{2+} sensitivity of g_{app} was estimated from the ratio of ATPase to force and computed from maximal ATPase activity, fiber volume and myosin concentration.

Experiment 2. The purpose of the second experiment was to determine if decreasing MgATP concentration alters g_{app}. Lowering MgATP concentration should reduce the rate at which XBs cycle from the WB to SB state by slowing the detachment of the rigor bond. Solutions were formulated such that a range of MgATP concentrations (0.25, 0.5, 1.0, 2.0 mM) were examined. Simultaneous measurements of isometric force

and myosin ATPase were made across the physiological range of Ca^{2+}. Estimates of the magnitude and Ca^{2+} sensitivity of g_{app} were determined as described in the detailed methods.

Specific Aim 2

The second aim of this investigation was to determine if g_{app} differs between fibers with known differences in XB cycling kinetics. If g_{app} is involved in the regulation of XB function one would expect it to differ between fast and slow fibers. Also, reducing [MgATP] should differentially affect g_{app} in fast and slow fibers.

Experiment 3. The purpose of the third experiment was to determine if differences in g_{app} exist between fast and slow fibers. Single muscle fibers were dissected from whole muscles which are known to contain either predominantly fast or slow fibers. Because frogs tend to have muscles of predominantly fast fibers, the rat model was used. Fast fibers were harvested from the extensor digitorum longus (EDL) and slow fibers from the soleus muscle of adult male Sprague Dawley rats. The fibers were chemically skinned and simultaneous measurements of isometric force and myosin ATPase were performed across a physiological range of Ca^{2+}. Estimates of the magnitude and Ca^{2+} sensitivity of g_{app} were made as described above.

Experiment 4. The aim of the fourth experiment was to determine if decreasing MgATP concentration alters g_{app} in both fast and slow fibers. Solutions were formulated such that MgATP concentrations of 0.5 and 2.0 mM were examined. Single muscle fibers

were dissected from whole soleus (slow) and EDL muscle (fast) and chemically skinned. Simultaneous measurements of isometric force and myosin ATPase were made across a physiological range of Ca^{2+}. The ATPase and force ratio was again used to estimate g_{app} as described in the detailed methods.

Specific Methods and Techniques

Solutions

Two stock solutions were made which differed in free-calcium concentration (Appendix I). These solutions contained 85 mM K^+ and Na^+, 1 mM Mg^{2+}, 7 mM ethylene glycol-bis(B-aminoethyl ether)-N,N,N,',N',-tetra acetic acid (EGTA), and propionate as the major anion. The standard Relaxing Solution contained no additional added calcium which resulted in a free calcium concentration of approximately 10^{-9} M or a pCa (-log free $[Ca^{2+}]$) of 9.0 while the Activating Solution contained added calcium to achieve a level of free Ca^{2+} of $10^{-4.5}$ M (pCa 4.5). Solutions were kept refrigerated and used within five days. On each experimental day 50 ml of each solution was placed on ice and the following constituents were added: ATP (varying), 0.4mM NADH, 5mM phosphoenol pyruvate (PEP), 100 U/ml pyruvate kinase (PK) and 140 U/ml lactate dehydrogenase (LDH). Myokinase activity was blocked by the addition of 0.2mM P1,P5-di(adenosine-5)pentaphosphate (AP_5A) (Guth & Wojciechowski, 1986).

Ionic strength of all solutions was adjusted to 0.18M and pH maintained at 7.0 with imidazole propionate. For solutions requiring altered [MgATP] and temperature,

constituent concentrations were adjusted to maintain the desired solution pH and free ion concentrations. (See appendix I) The concentrations of the ionic species were determined by a computer program kindly provided by Dr. Glenn Kerrick. Temperature was maintained at prescribed levels by one of three methods. A temperature of 20°C was achieved by equilibrating solutions to ambient room temperature. Temperature was reduced to 15°C by utilizing a water jacketed system to cool the gradient tubing leading to the cuvette. Further reductions in temperature (10°C) was realized by convective cooling in which compressed air was passed through a fine bore (2 mm) copper tubing submerged in an ice slurry and blown on the cuvette. Cuvette temperature for all three methods was periodically verified with a thermocouple wire probe placed in the cuvette. All chemicals for the experiments were obtained from Sigma Chemical Company.

Fiber dissection and skinning

For most experiments, muscle fibers were harvested from medium male grass frogs (*Rana pipiens*), (4-6cm, 20-30gm). Animals were anesthetized by submersion in an ice slurry for 10 minutes. At this point they were beheaded while in a cold-induced torpor. Semitendinosus muscles were harvested and immediately placed in a cold relaxing solution (pCa 9.0) with 50% glycerol (v/v) and 4 mM ATP added. Muscle bundles were then dissected free and placed in skinning solution for 20 minutes (relaxing solution containing 2mM ATP and 1% Triton X-100). Previous experience with this skinning protocol determined that force could be elicited by Ca^{2+} but not by caffeine, suggesting that both

the sarcolemma and the sarcoplasmic reticulum were disrupted (Williams et al., 1993; Williams & Ward, 1992).

Muscle fibers were also harvested from adult male Sprague Dawley rats (approximately 250-300g) and adult male Swiss Webster mice (55-65g). Following pentobarbital anesthesia (50mg/kg, IP), soleus and EDL muscles were harvested and fibers removed as described above. Animals were euthanized following the tissue harvesting by pentobarbital overdose (70 mg/kg, IP).

The procedures for the use of animals in these studies were approved by the Animal Use and Care Committee at Virginia Tech and are on file with the University Veterinarian.

Fiber mounting

After skinning, fiber bundles were transferred to a cold dissecting dish (60:40 relaxing solution/glycerol, 4 mM MgATP). Single fibers were dissected from the fiber bundle under a 15X stereo microscope. With the aid of microscopic video observation, fiber segments (2-3mm) were mounted between a pair of micro-tweezers in the Muscle Research System (Scientific Instruments GmbH) (Guth & Wojciechowski, 1986) (Figure 5). One pair of tweezers was attached to a photodiode force transducer (resolution 0.2mg at 5Hz, resonant frequency 1300Hz, output 10mg/V) and the other to a motorized length controller. The fiber was then placed in a quartz capillary with a cross-sectional area of $1mm^2$ and 1cm in length. Fiber slack length was determined by stretching the relaxed fiber.

Slack length was determined as the point at which increasing fiber length produced detectible force. Resting length was set by stretching fiber to 110% of slack length. This was predetermined to be an optimal length by previous experience with setting fiber length by laser diffraction analysis of sarcomere length of 2.5 μm.

Measurements

Following fiber mounting, the solution in the cuvette was illuminated by a high pressure xenon lamp with light filtered at 340nM. The video microscope was then removed and replaced with a microscope photometer and a 470 nM interference filter to allow the detection of NADH fluorescence in the solution.

Force-free Ca^{2+} relationships were determined by exposing the skinned fibers to a solution which contained incremental levels of free Ca^{2+} while monitoring isometric force. A gradient of Ca^{2+} was created with a calibrated gradient device (see below) in which solutions are perfused through the cuvette in 28μl increments. This procedure resulted in exposure to between 60-80 increments of Ca^{2+} between the range of pCa 9.0-4.5. The solution in the cuvette was exchanged every 15s which allowed sufficient time for increases in force to reach a steady plateau.

ATPase-free Ca^{2+} relationships were determined simultaneously with force production by a NADH fluorescence based coupled enzyme assay method (Loxdale, 1976; Guth & Wojciechowski, 1986; Kerrick et al. 1991). In this technique, ATP is regenerated from ADP and PEP by the enzyme pyruvate kinase (PK). This reaction is coupled to the

oxidation of NADH (fluorescent) to NAD (non-fluorescent) and the conversion of pyruvate to lactate by lactate dehydrogenase (LDH) as illustrated below.

ADP + PEP --------> ATP + pyruvate (catalyzed by PK)

pyruvate + NADH -------> lactate + NAD (catalyzed by LDH)

In this reaction, one mole of ADP, PEP and NADH is used to produce one mole of ATP, lactate and NAD. The rate of the decline in NADH fluorescence is converted to the rate of ATP hydrolysis by comparison to known standards. The solution in the cuvette was exchanged every 15s and the decline in fluorescence was determined over the last 10 seconds of the 15 second sample interval (See Figure 5).

Fiber Morphology

Following each individual fiber experiment, the fiber was removed from the cuvette and visualized with a calibrated video system. While briefly exposed to air, fiber diameter was determined on the video monitor with a mechanical micrometer (0.278 μm resolution). The smallest and largest diameters were measured and the points were averaged. Cross-sectional area (CSA) was computed assuming a cylindrical fiber shape. The force was normalized by CSA while ATPase activity was normalized by fiber volume to allow for direct comparison between fibers.

Gradient Device

The gradient device consisted of an upper chamber and a lower, mixing chamber.

Prior to each individual fiber experiment, 2.5ml of each stock solution was equilibrated to 20°C. Immediately prior to the experiment, ATP was added to the desired concentration (2.0, 1.0, 0.5, 0.25 mM). Relaxing solution was perfused into the device until the capillary, the tubing, and the 500µl lower mixing chamber was filled. The upper 2.5ml chamber was then filled with the activating solution. The lower mixing chamber was constantly stirred with a magnetic stir device.

The solution was perfused through the capillary with a peristaltic pump. With each pump step, 28µl of solution was withdrawn from the lower (low Ca^{2+}) chamber and replaced with 28µl of activating solution from the upper (high Ca^{2+}) chamber allowing gradual incremental increases in Ca^{2+}. The volume of the tubing and the amount delivered by the peristaltic pump were periodically calibrated. Free Ca^{2+} delivered to the cuvette with each pump step was computed via an algorithm provided by Dr. Konrad Güth. In addition Free Ca^{2+} was measured using the fluorescent indicator Calcium Green-2 (480nm excitation, 515 emission). Results of the Ca^{2+}calibration procedures are reported in Appendix II.

Data collection and Analysis

Isometric force and myosin ATPase activity during each step were collected via computer and analyzed off-line. The position and the shape ($[Ca^{2+}]_{50}$ and N) for the force and ATPase free Ca^{2+} relationship was determined by fitting the developed force and ATPase data obtained from each fiber to the modified Hill equation using a nonlinear

curve fitting routine (Sigma Plot, Jandel Scientific):

$$F/F_{max} = [Ca^{2+}]^N \cdot ([Ca^{2+}]_{50}{}^N + [Ca^{2+}]^N)^{-1}$$

where N is the slope of the relationship and $[Ca^{2+}]_{50}$ represents the Ca^{2+} concentration required to evoke 50% of maximal isometric force (F_{max}) or maximal ATPase activity (A_{max}). Statistical comparisons were made on the values for the $[Ca^{2+}]_{50}$ and N of the force and ATPase free-Ca^{2+} relationship.

Statistics

Analysis for statistical significance was conducted using one and two way ANOVA adjusted for repeated measures. Post-Hoc analysis was conducted using the Student Neuman Keuls method. Analysis was performed using Sigma Stat (Jandel Scientific). The significance for all analysis was set at the $p < 0.05$ level.

Results

Experiment 1

Raw force and NADH tracings collected during an individual fiber experiment are displayed in Figure 6. Data are from frog semitendinosus (ST) using 2.0 mM MgATP. It is apparent that both force and ATPase activity show graded increases with increasing Ca^{2+} until both reach a plateau. Additionally, increases in ATPase activity occur prior to detectable force output. Figure 6 also shows normalized force (F/F_{max}) and ATPase (A/A_{max}) values plotted against free Ca^{2+}. As can be seen, increased ATPase activity occurs at a lower $[Ca^{2+}]$ than does force output.

Mean values of F_{max}, A_{max}, $[Ca^{2+}]_{50}$ and slope (N) of force and ATPase curves of frog fibers (2 mM MgATP) can be found in Table 1. As noted, $[Ca^{2+}]_{50}$ and N values for force, ATPase were significantly different. Force and ATPase free Ca^{2+}curves generated from mean $[Ca^{2+}]_{50}$ and N values using the Hill equation are shown in Figure 7. According to Equation [7] A/F would remain constant if g_{app} did not vary as a function of free Ca^{2+}. Figure 7 clearly shows that A/F decreases by approximately 3 fold from pCa 5.78 to pCa 5.5 and remains constant below pCa 5.45. This decrease in A/F reflects the greater Ca^{2+} sensitivity of ATPase than force. It should be pointed out that in Figure 7 (as in all other figures displaying A/F), A/F was computed for pCa values where force was clearly detectible, that is greater than 10% of F_{max}.

Values for g_{app} in each fiber were calculated using Equation [7] and are presented in Figure 8. During maximal Ca^{2+} activation, g_{app} was calculated assuming $f_{app}/(f_{app}+g_{app}) = 0.95$ (Equation

1). This was determined based on the finding that maximal Ca^{2+} activated force could be increased by approximately 5% by including 10 mM MgADP in the activating solution and that further increases in [MgADP] caused no further increases in force. Inclusion of MgADP in the bathing solution is assumed to decrease XB dissociation such that the fraction of XBs in the SB state approaches 1.0. Therefore under normal conditions Fs ≈ 0.95. ATPase activity expressed as ATP hydrolyzed per myosin head was calculated by determining fiber volume and assuming 154 μM of myosin heads per liter (Ferenczi et al., 1984). The number of sarcomeres was calculated by using the known sarcomere spacing (2.5 μM) and fiber length . Based on these assumptions g_{app} at pCa 4.5 was 2.90±0.39 s^{-1}. At intermediate $[Ca^{2+}]$, g_{app} was computed from the A/F ratio using g_{app} measured at pCa 4.5.

It is possible that the Ca^{2+} sensitivity of g_{app} shown in Figure 8 is unique to frog skeletal muscle. To insure that such was not the case, measurements of force and ATPase activity were also performed on muscle fibers from fast EDL muscles from Sprague Dawley rats and Swiss Webster mice. Values for F_{max}, A_{max}, $[Ca^{2+}]_{50}$, and N of force and ATPase curves can be found in Table 2. Comparisons of force and ATPase $[Ca^{2+}]_{50}$ values within the rat and mice fibers showed significant differences supporting the results collected in the frog semitendinosus fibers. Force and ATPase versus pCa and ATPase/force versus pCa for all three species is shown in Figure 9. At pCa 4.5 g_{app} for rat and mouse were 3.13±0.35 and 5.77±0.27 s^{-1}, respectively. It is apparent that changes in A/F with increasing Ca^{2+} activation occur in several species.

As discussed in the Review of Literature, Brenner (1986) reported that the XB cycle was regulated primarily by f_{app} with g_{app} remaining insensitive across a range of intracellular free-Ca^{2+}.

He showed a linear relationship between ATPase and force which implies that the force and ATPase-free Ca^{2+} curves would superimpose. This is in contrast to the present data. A possible difference between the present study and that of Brenner (1986) is the experimental temperature at which the measurements are made (20° C versus 5° C). To investigate the possibility that the difference in experimental temperature accounts for the discrepant results, force and ATPase activity measurements were collected in frog semitendinosus muscle at 20, 15, and 10° C. Relationships between relative force and relative ATPase activity are shown in Figure 10. If g_{app} were insensitive to Ca^{2+} the plot of ATPase versus force would follow the line of identity (dashed line) in the graphic. That is, a change in force with increasing free [Ca^{2+}] would be matched by a proportional change in ATPase activity. It is apparent that at 21°C, ATPase and force are not linearly related. However, as temperature is reduced, the elevated ATPase activity at submaximal force output is diminished. In fact at 10°C, force and ATPase exhibit a near linear relationship similar to that reported by Brenner (1986). Thus, the contradictory findings between the present data and those of Brenner can be explained, in part, by different experimental temperatures.

Experiment 2

The effect of decreasing [MgATP] to 0.5 mM on the force and ATPase free Ca^{2+} curves is shown in Figure 11. A reduction in MgATP to 0.5 mM did not markedly alter the Ca^{2+} sensitivity of the ATPase curve but shifted the force curve to the left. This resulted in a smaller difference in Ca^{2+} sensitivity between force and ATPase.

Reducing [MgATP] markedly affected A_{max}. At 2.0 mM MgATP A_{max} was

419.67±56.24μM·s^{-1}. It was decreased to 242.92±10.34, 107.82±11.14, and 62.57±8.96μM·s^{-1} at 1.0, 0.5 and 0.25 mM MgATP, respectively. The effect of reduced [MgATP] on $[Ca^{2+}]_{50}$ and N for ATPase and force is seen in Figure 12. While no differences in N were seen in either force or ATPase with lowered MgATP, significant differences between force and ATPase $[Ca^{2+}]_{50}$ were seen at all [MgATP] except for 0.25 mM. While no changes in the $[Ca^{2+}]_{50}$ for ATPase activity occurred with reduced [MgATP], alterations in the $[Ca^{2+}]_{50}$ for force were seen. The $[Ca^{2+}]_{50}$ for force at 0.5 and 0.25 mM MgATP was significantly reduced compared to those recorded at 2.0 mM MgATP. Thus, as [MgATP] was decreased, the difference between the force and ATPase $[Ca^{2+}]_{50}$'s were progressively reduced as a result of a shift in the force-free Ca^{2+} curve towards the ATPase curve. Figure 13 shows the effects of reduced [MgATP] on the estimate for g_{app}. A fivefold decrease in g_{app} is seen at 2.0 mM MgATP and only a 2.5 fold decrease at 0.25 mM MgATP. It is clear that changes in magnitude and Ca^{2+} sensitivity of g_{app} occur as a result of decreasing [MgATP].

Experiment 3

As seen in Table 3, soleus and EDL fibers did not differ in F_{max} or the ATPase $[Ca^{2+}]_{50}$. They did however, differ in the force $[Ca^{2+}]_{50}$ and A_{max} with soleus fibers exhibiting a greater Ca^{2+} sensitivity to force and lower A_{max}. Comparison of the force and ATPase $[Ca^{2+}]_{50}$ values within each fiber type indicate that differences in force and ATPase Ca^{2+} sensitivity were smaller in soleus fibers. This appears to be due to differences in force $[Ca^{2+}]_{50}$.

Figure 14 displays the force and ATPase-free Ca^{2+} relationships in both EDL and soleus

fibers. It is apparent that the margin of separation between the force and ATPase curves is greater in the EDL fibers compared to the soleus fibers. These curves demonstrate that force but not ATPase of soleus fibers is more sensitive than the EDL to Ca^{2+}.

It is apparent that the ATPase to force ratios of the EDL fibers at submaximal levels of $Ca^{2+}$are substantially greater than those of soleus fibers (Figure 15). Calculated g_{app} values in EDL fibers show a six fold decrease in g_{app} across submaximal free Ca^{2+} levels while the soleus fibers exhibit a two fold decrease in g_{app}. At pCa 4.5, g_{app} of the EDL fibers was 3.13±0.35 s^{-1} compared to 1.50±0.04 s^{-1} for soleus fibers.

Experiment 4

The effects of reduced [MgATP] on the Ca^{2+} sensitivity of force and ATPase are shown in Figure 16. No significant differences were seen in the $[Ca^{2+}]_{50}$ of ATPase between 2.0 and 0.5 mM MgATP in either fiber type. However a reduction in [MgATP] to 0.5 mM resulted in a significant decrease in the $[Ca^{2+}]_{50}$ of force in the EDL fibers but not in the soleus fibers. In fact, reducing ATP abolished the difference in $[Ca^{2+}]_{50}$ for force between the soleus and EDL fibers.

Discussion

Specific Aim 1

The primary conclusion gained from Experiment One is that the kinetics of transition of the strong binding XBs to the WB state (i.e., g_{app}) is sensitive to changes in free Ca^{2+}concentration. Estimated values of g_{app} in fast fibers (frog, 2.0 mM MgATP, 20°C) are shown to decrease threefold from submaximal levels of Ca^{2+} (pCa 6.25) to maximal activating levels (pCa 4.5) (Figure 7). This conclusion is based on a model originally developed by Huxley (1957) and later modified by Brenner (1986) in which XBs cycle between SB and WB states (Figure 4.). The Ca^{2+} regulation of force in this model occurs via alterations in apparent rate constants f_{app} and g_{app} which represent the transition through the biochemical steps between these two states. Assuming that all of the available XBs are in this kinetic cycle throughout activation and that the average force per XB is constant (Brenner, 1986), the fraction of XBs in the force generating state determines the force output by the fiber. Thus force output is ultimately dependent on f_{app} and g_{app} which govern the transition from WB to SB and SB back to WB respectively.

Equation [2] defines XB force production as being proportional to the fraction of the cycling XBs in the SB state (F_s). In order for changes in force production to be ascribed to alterations in f_{app} and g_{app} two assumptions have been made. First, the average force per XB (F_{av}) must remain constant with Ca^{2+} activation. As noted earlier, Brenner (1988) has shown that S/F is equal to S_{av}/F_{av} and is constant across physiological levels of

calcium. Since it is highly unlikely that changes in F_{av} are matched by identical changes in S_{av} (thus keeping the ratio of S_{av}/F_{av} constant) it is accepted that these parameters remain constant through all levels of Ca^{2+} activation. With these results Brenner argued that the average force per XB remains unchanged with activation. Support for this conclusion has come from other authors who demonstrated that stiffness remains unchanged across activating levels of Ca^{2+} in rat soleus fibers at 15°C (McDonald & Fitts, 1995) and in rabbit psoas and rat vastus lateralis fibers at 15°C (Metzger & Moss, 1990). The second assumption is that the number of cycling XBs remain constant with activation. Brenner (1986, 1988) determined that the number of XBs in the kinetic cycle remains constant above 20% of maximal Ca^{2+} activation. Given these two assumptions, XB force must be regulated by the apparent rate constants f_{app} and g_{app}.

The ratio of myosin ATPase to isometric force was used to estimate g_{app} as described in equations [7] and [9]. It is evident that increasing free Ca^{2+} was associated with a sharp decline in g_{app} over submaximal levels of Ca^{2+} in all three species tested (Figure 9). These data contradict reports by Brenner (1986, 1988) who utilized rabbit psoas fibers (2.0mM MgATP, 5°C) and showed only slight alterations in g_{app} over a physiological range of free Ca^{2+}. The results of this investigation, however, support recent work by Kerrick et al. (1990) in which g_{app} was reported to be Ca^{2+} sensitive over submaximal levels of Ca^{2+} activation. Kerrick et al. (1990) reported pCa_{50} ($-\log[Ca]_{50}$) of ATPase and force to be 5.68 and 5.40 respectively in rabbit psoas muscle (2.0mM MgATP, 15°C). In this investigation $[Ca^{2+}]_{50}$ values for ATPase and force in rat EDL

fibers (2.0mM MgATP, 20°C) were 5.79 and 5.52. While the absolute values differ somewhat, differences between the ATPase and force pCa_{50}s were nearly identical (0.28 vs. 0.27 respectively). It is also important to note that calculations of ATP utilization per myosin head within muscle types (EDL, 2.0mM MgATP, 20°C, = 2.97 μmol·myosin $h^{-1}s^{-1}$) agree with those of Potma, VanGraas and Stienen (1994) (Psoas fibers, 2.0mM MgATP, 15°C, = 2.10 μmol·myosin $h^{-1}s^{-1}$) and Kerrick et al. (Psoas fibers, 2.0mM MgATP, 15°C, = 2.3 μmol·myosin $h^{-1}s^{-1}$)

In an attempt to explain the differing results between this investigation and that of Brenner et al. (1988), experiments were repeated at 20, 15 and 10°C in frog fibers (2.0mM MgATP) to determine the effect of experimental temperatures on estimates of g_{app}. If estimates for g_{app} were not Ca^{2+} sensitive, the plot of ATPase vs. force would be linear and fall on the dashed line as seen in Figure 10. It is evident (Figure 10) that lowering temperature resulted in a stepwise reduction in the ATPase activity such that at 10°C, the data is virtually insensitive to Ca^{2+} and similar to that reported by Brenner (1988). With this data, it can be argued that the discrepancies between the estimates of g_{app} can be at least partially explained by differences in experimental temperature.

A criticism which could be raised regarding the estimation of g_{app} by using the ratio of ATPase and force is that the lack of sarcomere length control during the experiments could overestimate the role of g_{app}. In fact, it is critical to estimates of g_{app} (Equation [2] and [4]) that the sarcomere length is controlled during the experiment. Unfortunately, the system used in this investigation does not allow for the simultaneous measurement of

sarcomere length and NADH fluorescence. However, the effect of not controlling sarcomere length on A/F in these experiments should be negligible. It has been demonstrated in this laboratory (personal observation, C.Ward) and by Kerrick et al. (1990) that the homogeneity of the laser diffraction pattern remains stable until force is greater than 50% of maximal and ATPase activity is greater than 90% of maximal. At this point the diffraction pattern becomes increasingly diffuse with increasing Ca^{2+} concentration. In these current experiments the majority of the change in g_{app} occurs below the $[Ca^{2+}]_{50}$ of force suggesting that the majority of g_{app} changes have been examined prior to any alterations in sarcomere length.

There are several implications for the contribution of g_{app} to XB force production. As shown in this investigation and that of Kerrick et al. (1990), g_{app} rapidly decreases at submaximal levels of Ca^{2+} (pCa 5.8-5.5) and remains constant above approximately pCa 5.5. As described in Equation [2], since n and F_{av} are assumed to be constant, isometric force can be calculated by the fraction of XBs (F_s) in the SB state. According to the mathematical relationship in Equation [2], a large g_{app} at the submaximal levels of Ca^{2+} decreases F_s by raising the level of the denominator. As g_{app} is rapidly decreased with increased Ca^{2+}activation, the contribution of g_{app} to the denominator is rapidly reduced thereby increasing the F_s independent of any changes in f_{app}. It is important to note however, that in a physiological system g_{app} and f_{app} would be expected to be somewhat interdependent. In this model, the contribution of g_{app} to forces near maximal Ca^{2+} activation is minimal due to both the overwhelming influence of f_{app} and the relative stable

contribution of g_{app} at near maximal levels of Ca^{2+}.

Experiment Two was designed to determine if lowering [MgATP] would decrease g_{app} as predicted in the biochemical model of the XB cycle (Figure 3). The effects of 2.0 and 0.5 mM [MgATP] on the force and ATPase free-Ca^{2+} relationship are seen in Figure 11. These data are similar to that of Kerrick et al. (1990) in which a similar narrowing of the ATPase and force-free Ca^{2+} was seen with reduced [MgATP]. Two other concentrations of [MgATP] were also used to determine if a MgATP concentration dependent relationship existed. While the $[Ca^{2+}]_{50}$ for ATPase was relatively unaffected by lower [MgATP] the $[Ca^{2+}]_{50}$ for force was significantly altered at 0.25mM and 0.5mM when compared to 2.0 mM. This resulted in the narrowing of the difference between the ATPase and free Ca^{2+} curves (Figure 12) and a stepwise decrease in the estimate for g_{app} (Figure 13). These data support the prediction that reduced [MgATP] will affect the contribution of g_{app} in the XB cycle.

Examination of the mathematical models used to probe the XB cycle offer support for the findings in Experiment Two. With the assumptions that the number of the XBs in the kinetic cycle and the force per XB remain constant with Ca^{2+} activation, equations for force, ATPase, and k_tr can be summarized as follows:

$$\text{Force} \propto [f_{app}/(f_{app}+g_{app})]$$

$$\text{ATPase activity} \propto [g_{app} \cdot f_{app}/(f_{app}+g_{app})]$$

$$k_{tr} \propto f_{app} + g_{app}$$

Reductions in [MgATP] to 0.5 mM were shown to decrease the magnitude of g_{app} at submaximal levels of Ca^{2+} resulting in increased isometric force and reduced ATPase activity at pCa 6.0 in fast fibers (Figure 11 and Kerrick et al. 1990). Examination of the ratiometric relationship between f_{app} and g_{app} in contributing to force and ATPase activity shows that only changes in g_{app} satisfy both of these alterations in force and ATPase. Similarly, Brenner's (1986) report that reduced [MgATP] (0.2 mM) did little to affect k_{tr} at maximal Ca^{2+} activation is not surprising since g_{app} remains constant below pCa 5.5 in fast fibers. Since f_{app} increases with increasing Ca^{2+} activation, changes in f_{app} may explain the increases in force but cannot explain both the reductions seen in ATPase activity, and the unaltered k_{tr} associated with decreased [MgATP]. Therefore the changes in the $[Ca^{2+}]_{50}$ of force due to lowered [MgATP] must be the result of g_{app}.

Specific Aim 2

Since g_{app} was found to be Ca^{2+} sensitive and most likely played a role in XB force production in fast fibers of the rabbit (Kerrick 1990), frog, rat and mouse, it was hypothesized that muscles with differing contractile characteristics would most likely have differing estimates for the contribution of g_{app}. As mentioned previously, contractile differences between fiber types manifest in slow fibers having decreased sensitivity and reduced slope of the force-free Ca^{2+}relationship when compared to fast fibers. In Experiment Three, estimates of g_{app} were compared between fast (EDL) and slow fibers

(soleus) of the rat at 20°C (2.0mM MgATP). Figure 14 and 15 display the force and ATPase free-Ca^{2+} relationship and the estimates for g_{app} respectively. Force and ATPase curves are closer together in the slow fibers compared to the fast fibers. Thus, fast fibers show a greater decrease in the estimate for g_{app} across levels of free-Ca^{2+}. In fact calculated values for g_{app} decline two fold in the soleus fibers while declining over six fold in the EDL fibers.

Similar results to the soleus data reported here were described by Krasner and Kushmerick (1983). These authors showed that relative ATPase and force data in soleus fibers nearly superimpose resulting in an extremely low A/F in the soleus with increasing Ca^{2+} activation.

Contractile differences between fast and slow fibers found in this investigation can also be predicted by alterations in the ratiometric relationship of g_{app} and f_{app} (as outlined in the equations above). As described previously, fast fibers show a decreased force, increased ATPase activity, and increased k_{tr} when compared to slow fibers. Only increases in g_{app} can satisfy all three conditions.

The effect of decreased [MgATP] on the Ca^{2+} sensitivity of force and ATPase is shown in Figure 16. Decreasing [MgATP] to 0.5 mM did not alter the $[Ca^{2+}]_{50}$ of ATPase in either the EDL or soleus. Reduced [MgATP] did however reduce the $[Ca^{2+}]_{50}$ for force in the EDL fibers while having no effect on the soleus fibers. It is interesting to note that the reduction in [MgATP] to 0.5 mM eliminated the differences in the $[Ca^{2+}]_{50}$ of force between the EDL and soleus fibers. While this finding supports the results of Experiment

Two, it also strongly suggests that differences in the Ca^{2+}sensitivity between fast and slow fibers can be attributed, at least in part, to different contributions of g_{app}.

General Conclusions and Recommendations

As evidenced by the results of this investigation, g_{app} decreases with increasing levels of submaximal free-Ca^{2+} in both fast and slow fibers. This Ca^{2+} sensitivity of g_{app} supports a role for this apparent rate kinetic in the regulation of force at the XB. While the magnitude of A/F (estimate of g_{app}) was seen to be quite large at 20°C, it is apparent that changes in temperature affect A/F to a great extent (Figure 10). With this data one could speculate that the magnitude of g_{app} at more physiological temperatures (i.e., 37°C) would likely be increased. Thus any contribution of g_{app} to XB force regulation would be increased at physiological temperatures.

While no measurements of f_{app} were made in this investigation, those reported by Brenner (1988) can be used to obtain a view of the interaction of f_{app} and g_{app}. For example, in fast fibers, the majority of g_{app}'s contribution to XB force regulation would occur at isometric forces below 40% of F_{max} (pCa 5.5) (Figure 14 and 15). Brenner (1988) showed that the majority of the increase in f_{app} in fast fibers occurred above 40% of isometric force. It is interesting to speculate that if the findings of f_{app} seen by Brenner are combined with the findings of g_{app} seen in this investigation, it is plausible that the interaction of f_{app} and g_{app} could provide more sensitive control of XB cycling across a wider physiological range of Ca^{2+} than each could individually.

Recommendations for Future Research

The findings in this investigation contribute to the scientific body of knowledge in the area of the contractile force regulation in skeletal muscle. Investigations into XB cycling kinetics provides the basis for understanding alterations in contractile performance.

Much information would be gained by characterizing both f_{app} and g_{app} in the experimental conditions of this investigation. While results have independently demonstrated roles for f_{app} and g_{app}, a single investigation which explores the interaction of these Ca^{2+} sensitive apparent rate constants has not been conducted. These data would provide further understanding of force regulation at the XB level.

Important experiments in XB function have been conducted by manipulating or replacing regulatory proteins involved in the XB cycle. Extraction and re-addition of myosin LC2 and Tn-C have been powerful tools in investigating the XB cycle and have provided valuable information on the regulatory mechanisms of the XB cycle. Much information would be gained by investigating the role of f_{app} and g_{app} with these manipulations. With this data, precise regulatory contributions of the apparent rate constants could be explored.

A multitude of situations exists whereby contractile performance is altered in skeletal muscle. These include metabolic perturbation (e.g., pH, P_i, oxidative stress, etc.) as well as changes in force elicited by activity, inactivity and disease states (e.g., fatigue, hypertrophy and atrophy). Many situations also exist where a subtle change in muscle

chemistry effects the contractile performance of muscle. For example, solutions which were altered to mimic a fatigued intracellular milieu (Godt and Nosek, 1989) were shown to alter contractile performance. Subsequent investigations involving the effects of reduced pH on myofibrillar ATPase activity (Potma, Vangraas, and Steinen, 1994) and k_{tr} (Metzger and Moss, 1990) have also shown alterations with altered pH. In order to understand the mechanisms underlying these changes it is important to examine the fundamental functioning of the XB cycle (f_{app} & g_{app}). While several experiments have been performed which have used values of k_{tr} to investigate the functioning of the XB cycle, data presented in this investigation suggest that important information might be gained by further examining the contributions of f_{app} and g_{app}.

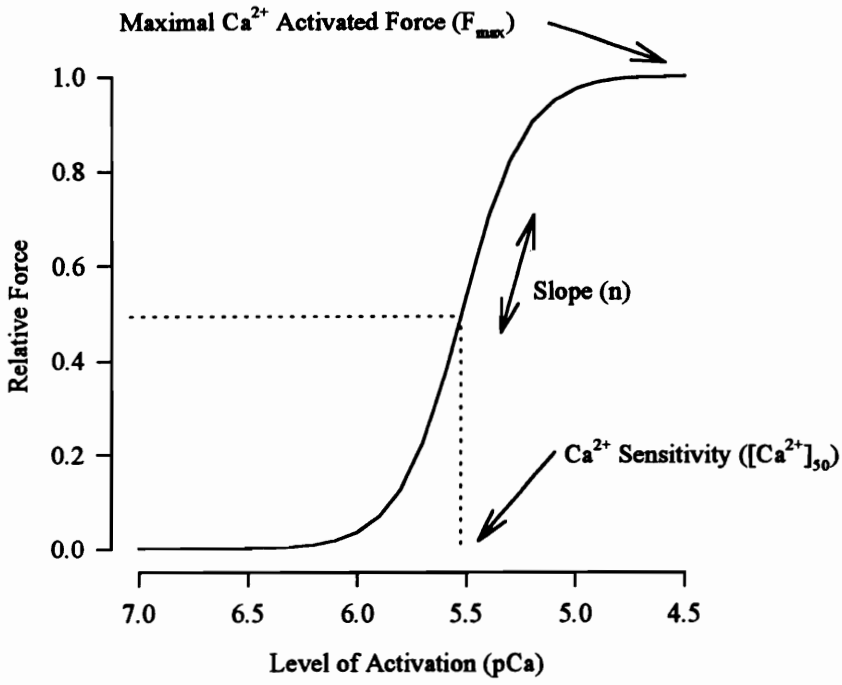

Figure 1. The relationship between force and free $[Ca^{2+}]$. Relative force is calculated as F/F_{max}. Thus 1.0 is equal to 100% of F_{max}.

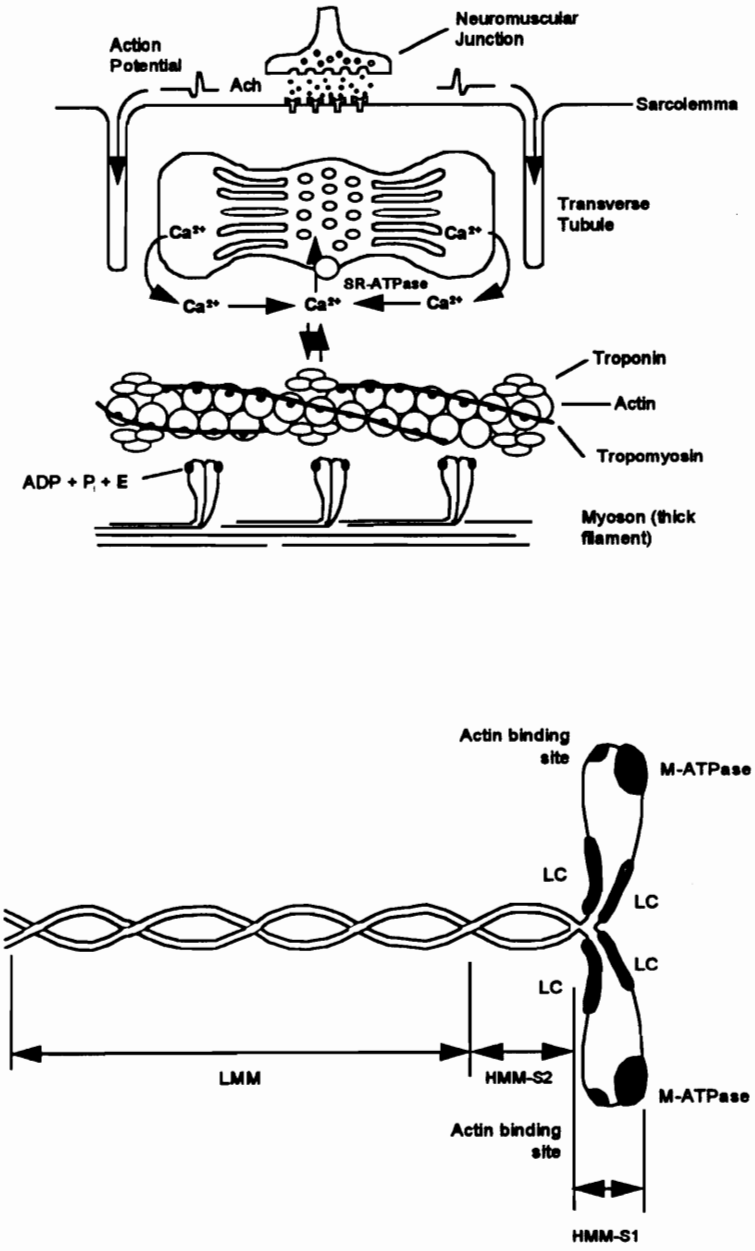

Figure 2. Schematic representation of the structures involved in the skeletal muscle excitation-contraction process (Top). Diagram of the myosin molecule (Bottom).

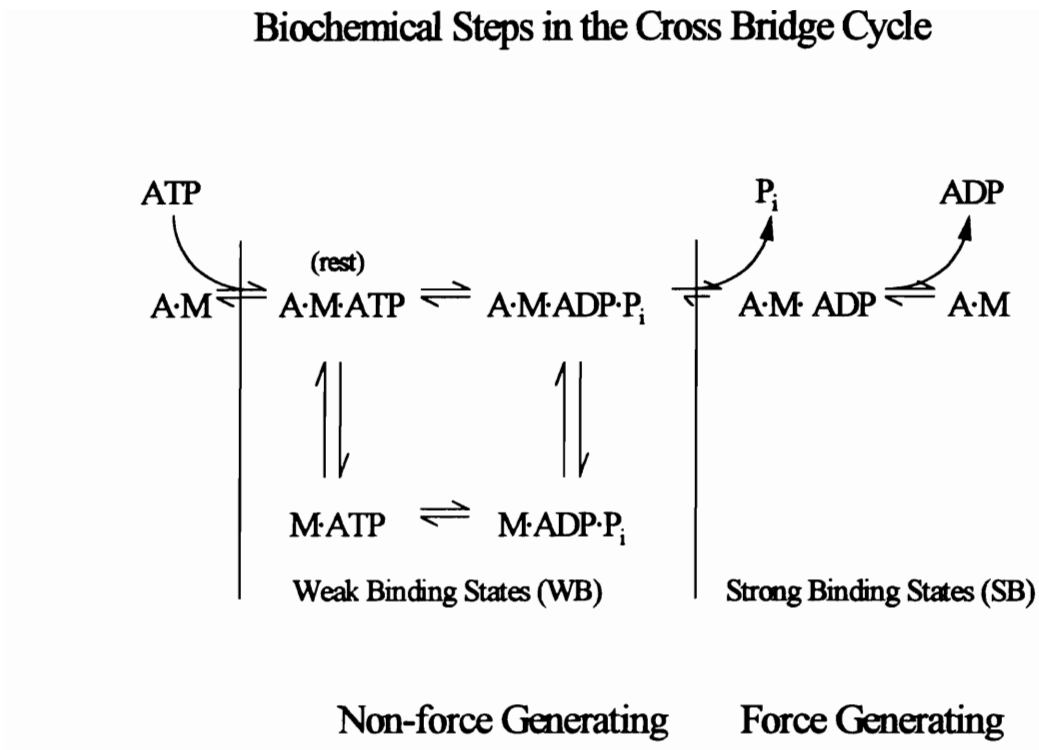

Figure 3. Biochemical model of actin (A) and myosin (M) interaction in solution. Adapted from Stein et al. (1979). Symbol (·) denotes a bound state, e.g., A·M denotes actin and myosin bound.

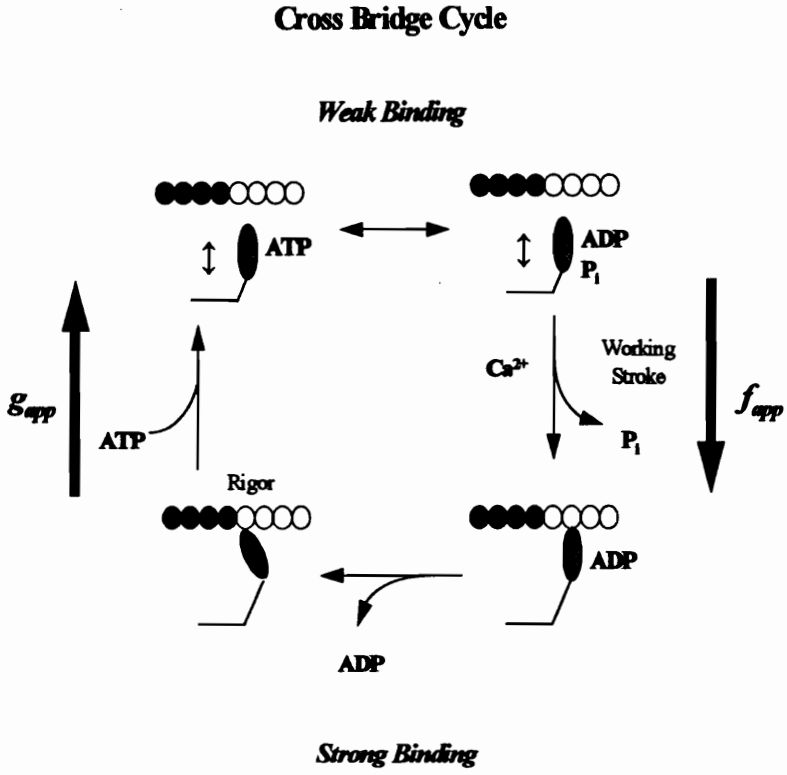

Figure 4. Diagrammatic representation of the cross-bridge cycle. The apparent rate constants f_{app} and g_{app} represent the transition through a number of biochemical steps between the weak binding and strong binding states.

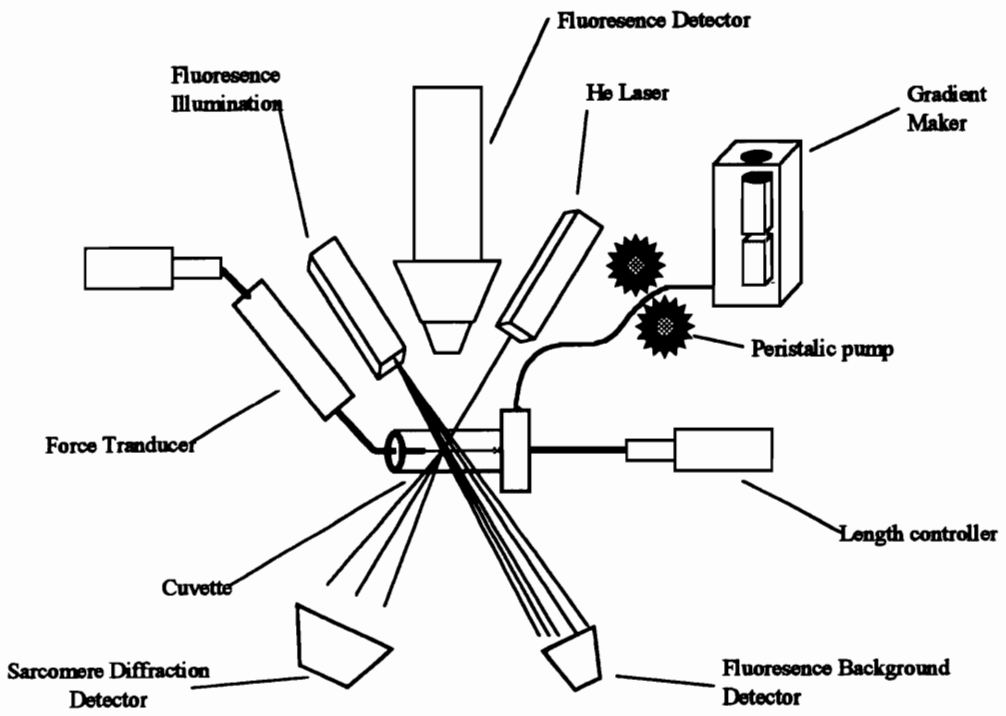

Figure 5. Schematic diagram of the Muscle Research System (Scientific Instruments GmbH).

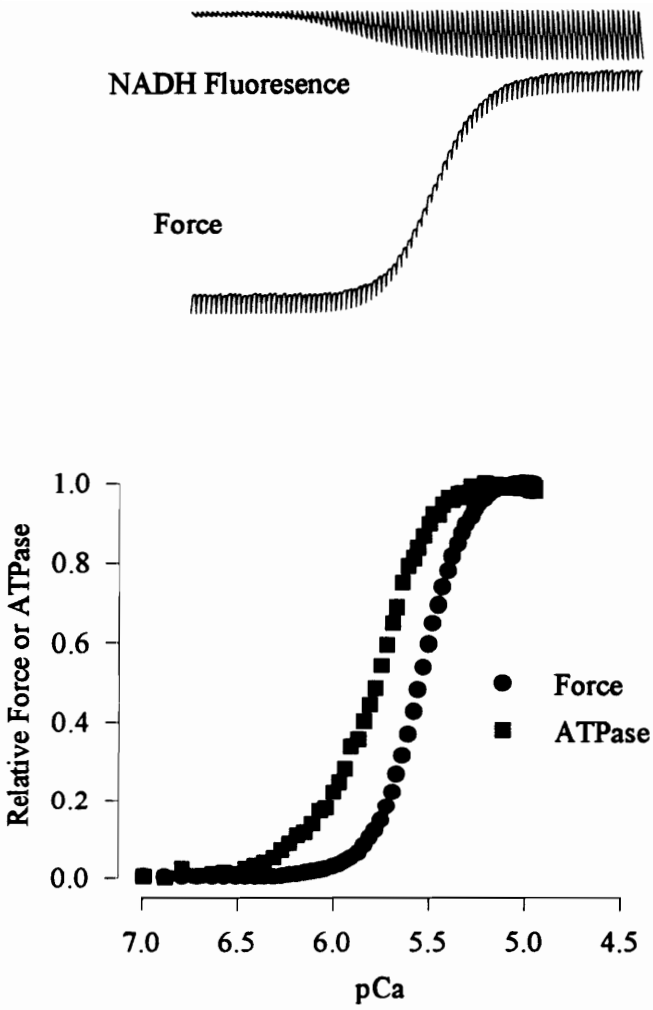

Figure 6. Measurement of ATPase-free Ca^{2+} and force-free Ca^{2+} relationships. Shown are raw tracing of NADH and force (top) with increasing Ca^{2+} activation and normalized force and ATPase values vs. free-Ca^{2+} (bottom).

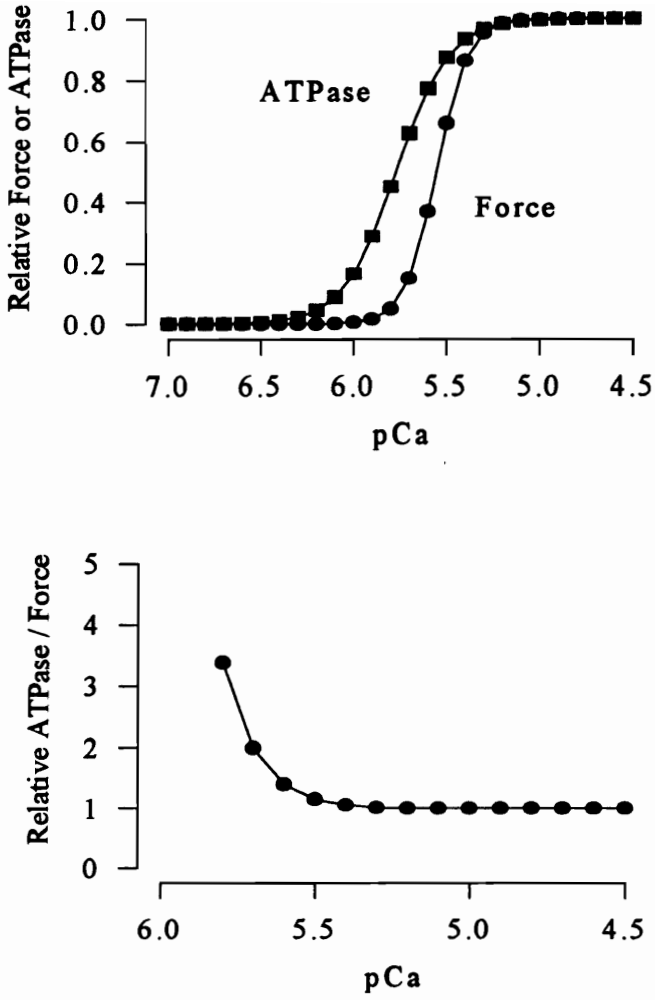

Figure 7. Relationships between force, ATPase activity and free $[Ca^{2+}]$ (top). $[Ca^{2+}]_{50}$ for force and ATPase were significantly different (2.64±0.14 and 1.586±0.08 μM respectively. $p < 0.05$). ATPase and force ratio vs. free $[Ca^{2+}]$ (bottom). Data are mean values from frog fibers, 2.0 mM MgATP (n=9).

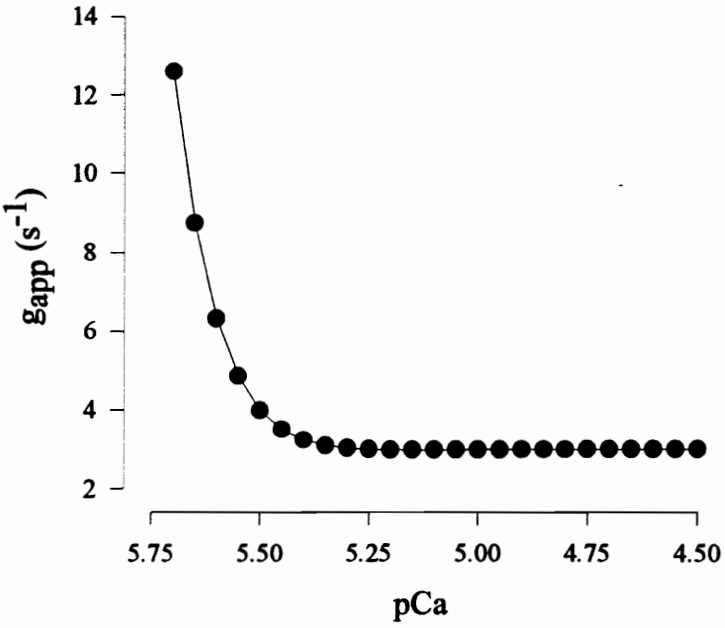

Figure 8. Calculated g_{app} values vs. free Ca^{2+} (Frog fibers 2.0 mM MgATP, n=9). g_{app} at pCa 4.5 = 2.90±0.39 s^{-1}.

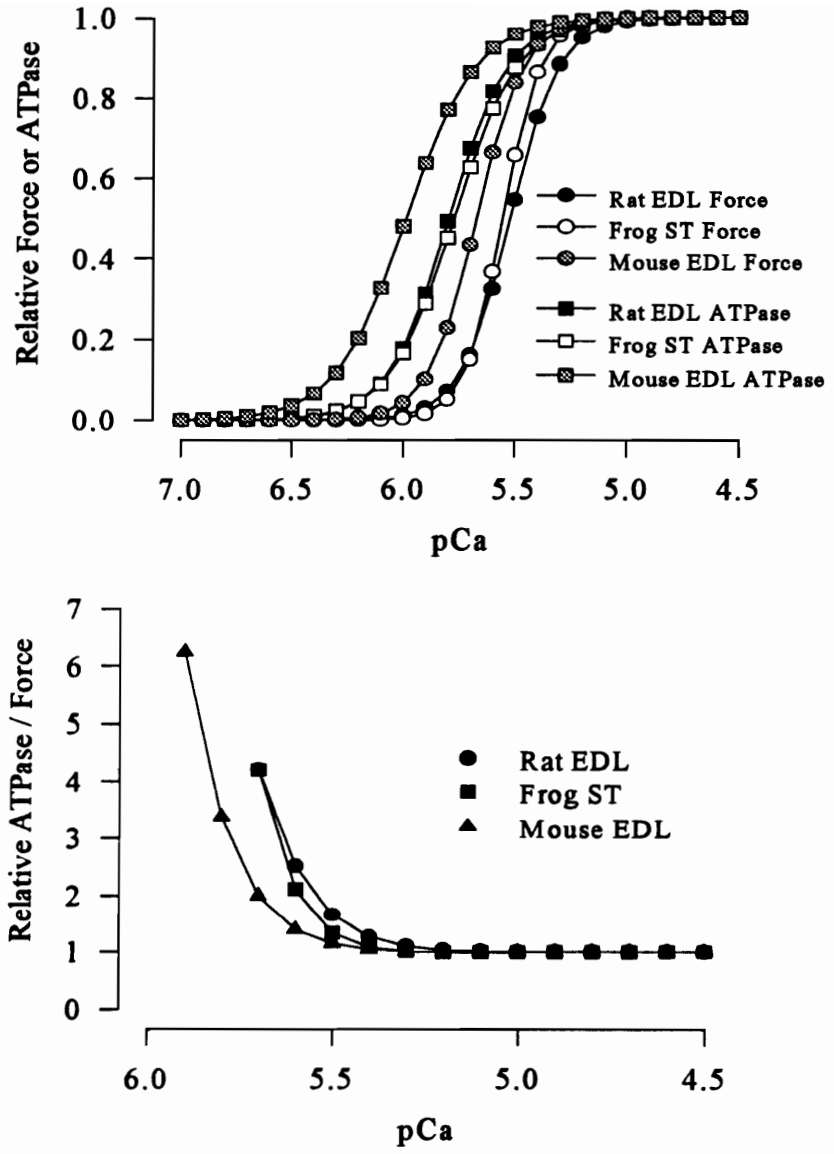

Figure 9. Relative Force and Relative ATPase free-Ca^{2+} curves for three animal species (2.0 mM MgATP) (top). ATPase to force ratio for each species (bottom).

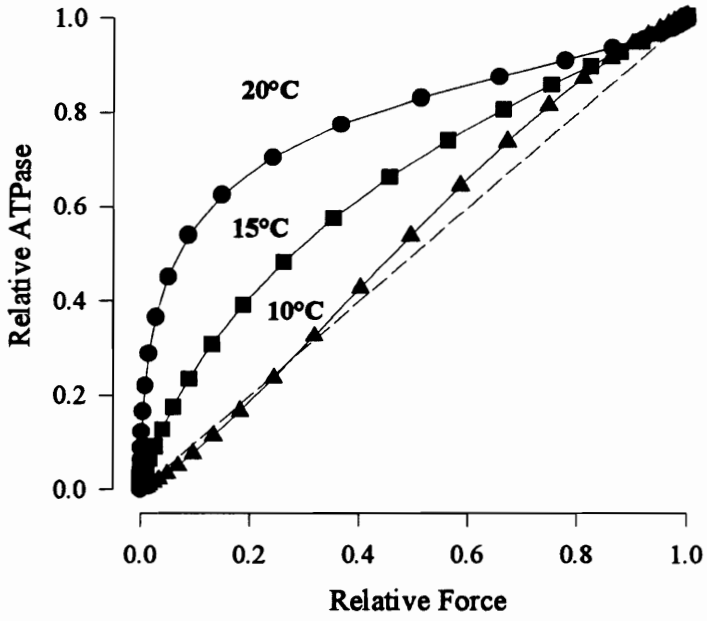

Figure 10. Relationships between relative force and relative ATPase activity recorded at 20, 15 and 10°C in frog ST fibers.

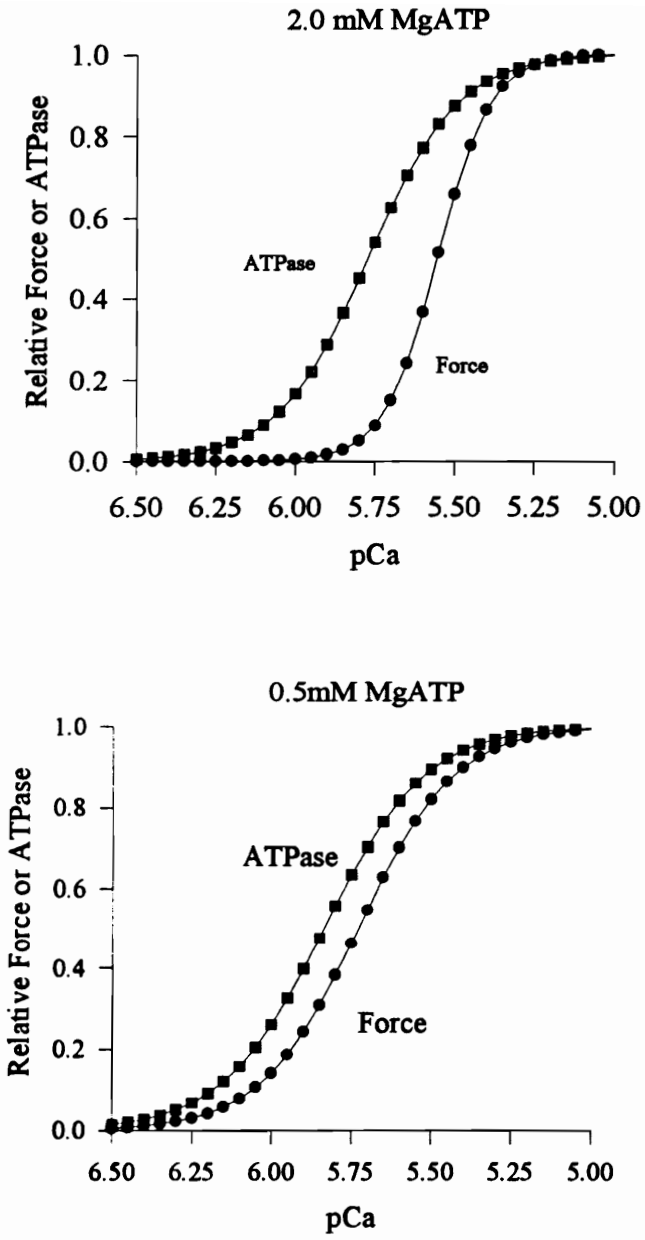

Figure 11. Relative force and ATPase free-Ca^{2+} curves collected at 2.0 (top, n=9) and 0.5 (bottom, n=6) mM MgATP in frog fibers (20°C).

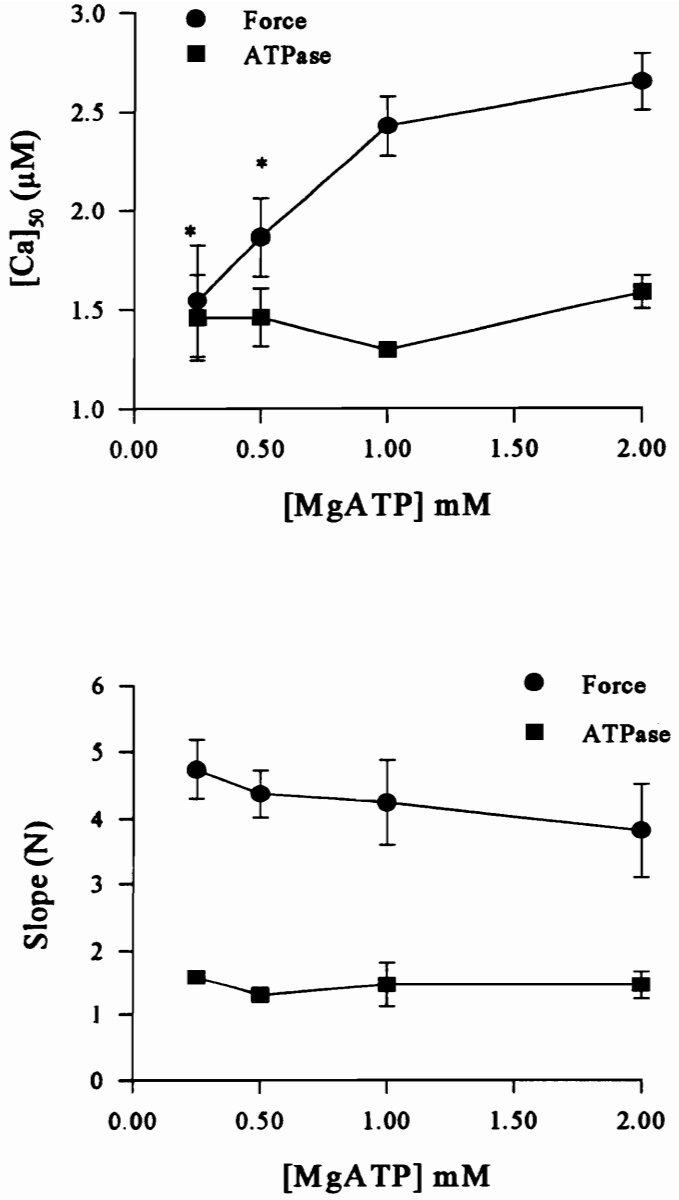

Figure 12. $[Ca^{2+}]_{50}$ (top) and slope (N) (bottom) values for force and ATPase free Ca^{2+} curves in frog ST fibers at 2.0, 1.0, 0.5, 0.25 mM MgATP (*$p < 0.05$ vs.2.0 mM) .

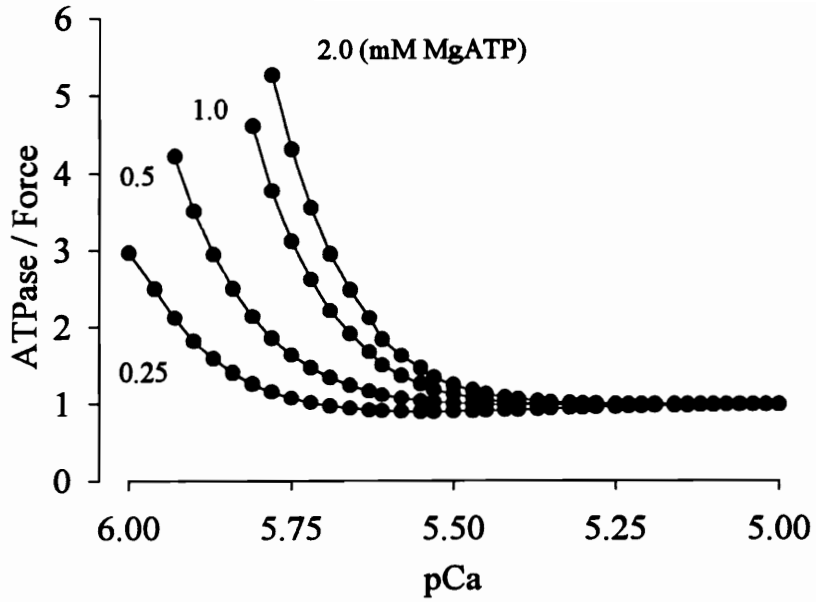

Figure 13. ATPase vs. force ratios at varying MgATP concentrations in frog ST fibers (20°C).

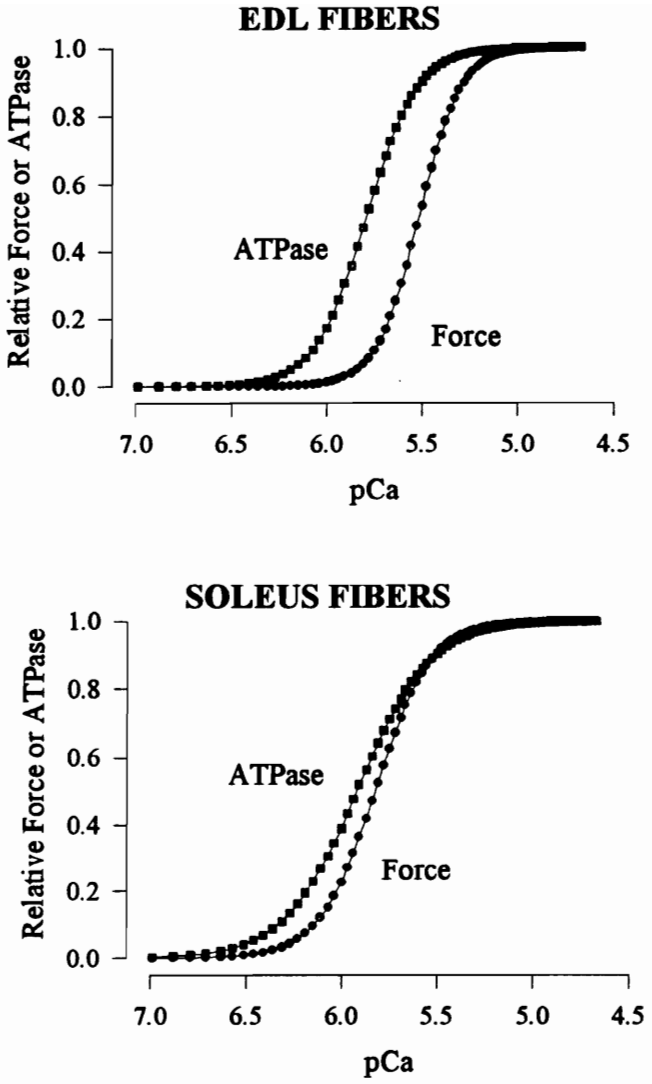

Figure 14. Force and ATPase free-Ca^{2+} relationships between rat EDL (n=7) and soleus (n=9) fibers (2.0 mM MgATP, 20°C).

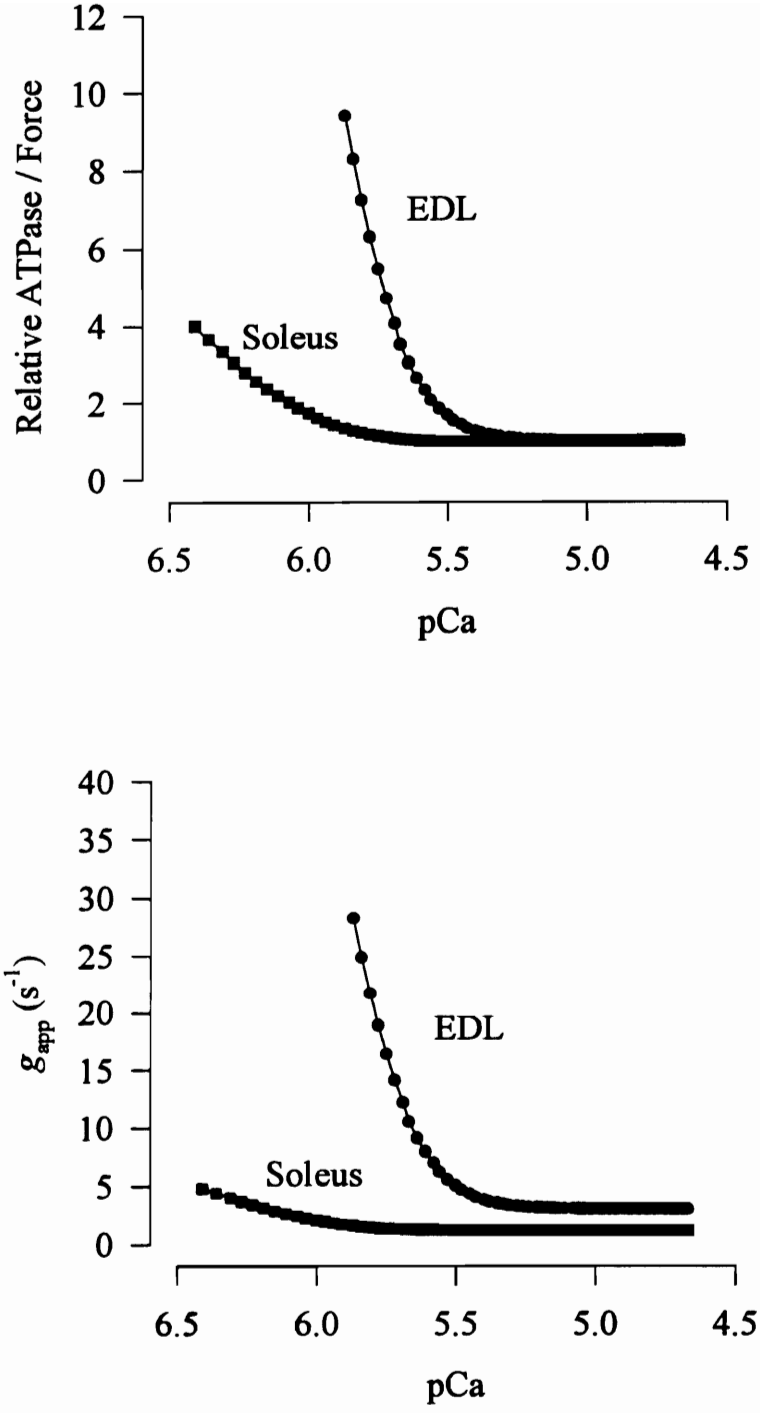

Figure 15. ATPase to force ratio between soleus and EDL fibers (top). Calculated values for g_{app} between EDL and soleus fibers (bottom).

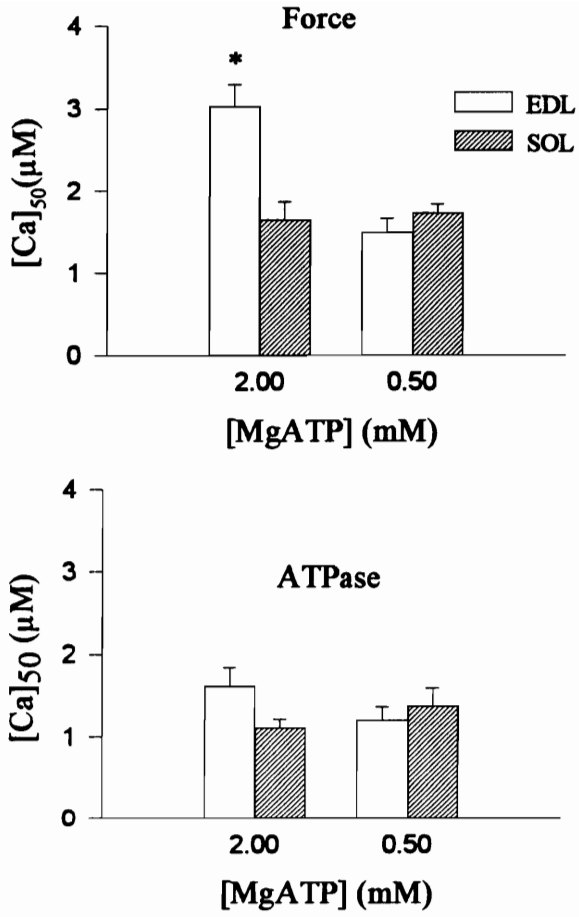

Figure 16. $[Ca^{2+}]_{50}$ values for force between EDL and soleus fibers (top). $[Ca^{2+}]_{50}$ values for ATPase between EDL and soleus fibers (bottom) (* $p<0.05$ vs. SOL and vs.0.5 mM).

TABLE 1

Force			ATPase Activity		
F_{max} ($kN \cdot m^{-2}$)	$[Ca^{2+}]_{50}$ (μM)	N	A_{max} ($\mu M \cdot s^{-1}$)	$[Ca^{2+}]_{50}$ (μM)	N
60.42± 8.12	2.64±0.14*	4.74±.45*	419.67±56.24	1.58±0.08	2.85±0.23

Frog Semitendinosis fibers (2.0 mM [MgATP], 20°C) (n=9)
(* denotes difference from ATPase value, $p<0.05$)

TABLE 2

	Force			ATPase Activity		
	F_{max} ($kN \cdot m^{-2}$)	$[Ca^{2+}]_{50}$ (μM)	N	A_{max} ($\mu M \cdot s^{-1}$)	$[Ca^{2+}]_{50}$ (μM)	N
Rat	92.91±3.18	3.02±0.27*	3.97±0.26	457.64±51.33	1.61±0.24	3.28±0.42
Mouse	112.75±4.16	2.13±0.03*	4.14±0.06*	843.92±39.89	1.03±0.02	2.80±0.08

Rat (n=7) and mouse (n=10) EDL fibers (2.0 mM [MgATP], 20°C)
(* denotes difference from ATPase value, $p<0.05$)

TABLE 3

	Force			ATPase Activity		
	F_{max} ($kN \cdot m^{-2}$)	$[Ca^{2+}]_{50}$ (μM)	N	A_{max} ($\mu M \cdot s^{-1}$)	$[Ca^{2+}]_{50}$ (μM)	N
Soleus	96.03±8.67	1.48±0.17#	3.03±0.19	219.36±6.23#	1.20±0.16	2.33±0.13#
EDL	92.91±3.18	3.02±0.27*	3.97±0.26	457.64±51.33	1.61±0.24	3.28±0.42

Rat soleus (n=9) and EDL (n=7) fibers (2.0 mM [MgATP], 20°C)
(* denotes difference from ATPase value within muscle , $p<0.05$)
(# denotes difference between muscle types , $p<0.05$)

LITERATURE CITED

Bagshaw C.R., J.F. Eccleston, F. Eckstein and F. Goody, Two step process of adenosine triphosphate association and adenosine diphosphate dissociation. *Biochemical Journal* 141:351-364, 1974.

Berne R.M. and M.N. Levy, *Physiology* C.V Mosby Company, 315-343, 1988.

Bottinelli, B., M. Canepari, C. Reggiani and G.J.M. Stienen, Myofibrillar ATPase activity during isometric contraction and isomyosin composition in rat single skinned muscle fibers. *Journal of Physiology* 2972: 663-675, 1994.

Brandt P.W., M.S. Diamond and F.H. Schachat, The thin filament of vertebrate skeletal muscle co-operatively acts as a unit. *Journal of Molecular Biology* 180: 379-384, 1984.

Brandt P.W., M.S. Diamond, J.D. Rutchik and F.H. Schachat, Co-operative interactions between troponin-tropomyosin units extend the length of the actin filament in skeletal muscle. *Journal of Molecular Biology* 195: 885-896, 1987.

Bremel R.D. and A. Weber, Cooperation within actin filament in vertebrate skeletal muscle. *Nature New Biology* 238:97-101, 1972.

Brenner B., The cross-bridge cycle in muscle. Mechanical, biochemical, and structural studies on skinned rabbit psoas fibers to characterize cross-bridge kinetics in muscle for correlation with the actomyosin-ATPase in solution. *Basic Research in Cardiology* 81: 1-15, 1986.

Brenner B. and E. Eisenberg, Rate of force generation in muscle: correlation with actomyosin ATPase in solution. *Proceedings of the national Academy of Sciences* Vol 83, 3543-3546, 1986.

Brenner B., Mechanical and structural approaches to correlation of cross-bridge action in muscle with actomyosin ATPase in solution. *Annual Review of Physiology* 49:655-672, 1987.

Brenner B., Effect of Ca^{2+} on cross-bridge turnover kinetics in skinned single rabbit psoas fibers: implications for regulation of muscle contraction. *Proceedings of the National Academy of Sciences* 85: 3265-3269, 1988.

Chalovich J.M., L.C. Yu and B. Brenner, Involvement of weak binding cross-bridges in force production in muscle. *Journal of Muscle Research and Cell Motility* 12, 503-506, 1991.

Cooke R. and E. Pate, The effects of ADP and phosphate on the contraction of muscle fibers. *Biophysical Journal* Vol. 48, 789-798, 1985.

Cooke R., Franks K., G.B. Lucciani and E. Pate, The inhibition of rabbit skeletal muscle contraction by hydrogen ions and phosphate. *Journal of Physiology* 395, 77-97, 1988.

Donaldson S.K.B. and L. Hermansen, Differential, direct effects of H^+ on Ca^{2+}-activated force of skinned fibers from the soleus, cardiac and adductor magnus muscles of rabbits. *Pflügers Archives* 376, 55-65, 1978.

Eaton B., Structural changes during activation of skeletal muscle *Science*, 192:1337-1339, 1976.

Eisenberg E. and C. Moos, The ATPase activity of acto-heavy meromyosin: a kinetic analysis of actin activation. *Biochemistry* 7:1486-1489, 1968.

Eisenberg E., C.R. Zobel and C. Moos, Subfragment 1 of myosin:adenosine triphosphatase activation by actin. *Biochemistry* 7:3186-3194, 1968.

Fabiato A. and F. Fabiato, Effects of pH on the myofilaments and sarcoplasmic reticulum of skinned cells from cardiac and skeletal muscles. *Journal of Physiology (London)*, 276: 233-255, 1978.

Gardetto P.R., J.M. Schluter and R.H. Fitts, Contractile function of single muscle fibers after hind limb suspension. *Journal of Applied Physiology*, 66: 2739-2749, 1989.

Gillis J.M. and E.J. O'Brien, Structural differences between rested and rigored muscle. *Journal of Molecular Biology*, 99:445-459, 1975.

Godt R.E. and T.M. Nosek, Changes in the intracellular milieu with fatigue or hypoxia depress contraction of skinned rabbit skeletal and cardiac muscle. *Journal of Physiology (London)* 412: 155-180, 1989.

Guth K. and R. Wojciechowski, Perfusion cuvette for the simultaneous measurement of mechanical, optical and energetic parameters of skinned muscle fibers. *Pflugers Archives* 407, 522-527, 1986.

Higuchi H., Y.E. Goldman, Sliding distance per ATP hydrolyzed by myosin heads during isotonic shortening of skinned muscle fibers. *Biophysical Journal* 69: 1491-1507, 1995.

Hill A.V., *The Living Machinery* Harcourt, Brace and Company, 1927

Hoffman P.A., J.M. Metzger, M.L. Greaser and R.L. Moss, Effects of partial extraction of light chain 2 on the Ca^{2+} sensitivities of isometric tension, stiffness, and velocity of shortening in skinned skeletal muscle fibers. *Journal of General Physiology* 95:477-497, 1990.

Huchet C. and C. Leoty, Calcium sensitivity of skinned ferret EDL, soleus, and cremaster fibers. *American Journal of Physiology* 264: R867-R870, 1993.

Huxley A.F., Muscle structure and theories of contraction. *Progress in Biophysics and Biophysical Chemistry*, 7:255-318, 1957.

Huxley H.E. and R.M. Simmons, Proposed mechanism of force generation in striated muscle. *Nature* 233: 533-538, 1971.

Kandarian S.C. and J.H. Williams, Contractile properties of skinned fibers from hypertrophied skeletal muscle. *Medicine and Science in Sports and Exercise* 25: 999-1004, 1993

Kerrick W.L., J.D. Potter and P.E. Hoar The apparent rate constant for the dissociation of force generating myosin crossbridges from actin decreases during Ca^{2+} activation of skinned muscle fibers. *Journal of Muscle Research and Cell Motility*, 12, 53-60, 1991.

Krashner B.H. and M.J. Kushmerick, Tension and ATPase rate in steady-state contractions of rabbit soleus fiber segments. *American Journal of Physiology (Cell Physiology), 14*: C405-C414, 1983.

Kraft T., J.M. Chalovich, L.C. Yu and B. Brenner, Parallel inhibition of active force and relaxed fiber stiffness by caldesmon fragments at physiological ionic strength and temperature conditions: additional evidence the weak binding cross-bridge binding to actin is an essential intermediate for force generation. *Biophysical Journal,* 68: 2404-2418, 1995.

Loxdale H.D. A method for the continuous assay of picomole quantities of ADP released from glycerol-extracted skeletal muscle fibers on MgATP activation. *Journal of Physiology,* 260: 4, 1976.

Lymn R. W. and E.W. Taylor, Mechanism of adenosine triphosphate hydrolysis by actomyosin. *Biochemistry* 10:4617-4624, 1971.

Needham D.M., *Machina Carnis: The Biochemistry of Muscular Contraction in its Historical Development* Cambridge University Press, 1971

Manning D.R. and J.T. Stull, Myosin light chain phosphorylation-dephosphorylation in mammalian skeletal muscle, *Americal Journal of Physiology* 242: C234-C241, 1982.

McDonald K.S. and R.H. Fitts, Effect of hind limb unloading on rat soleus fiber force, stiffness and calcium sensitivity. *Journal of Applied Physiology* 79: 1796-1802, 1995.

Metzger J.M. and R.L. Moss, Greater hydrogen ion-induced depression of tension and velocity in skinned single fibers of rat fast than slow muscles. *Journal of Physiology* 393, 727-742, 1987

Metzger J.M. and R.L. Moss, Calcium sensitive cross-bridge transitions in mammalian fast and slow skeletal muscle fibers. *Science*, 247: 1088-1090, 1990.

Metzger J.M. and R.L. Moss, pH modulation of the kinetics of a Ca^{2+} sensitive cross-bridge state transition in mammalian single skeletal muscle fibers. *Journal of Physiology* 428, 751-764, 1990.

Metzger J.M., M.L. Greaser and R.L. Moss, Variations in cross-bridge attachment rate and tension with phosphorylation of myosin in mammalian skinned skeletal muscle fibers. *The Journal of General Physiology*, 93: 855-883, 1989.

Moss R.R., Ca^{2+} regulation of mechanical properties of striated muscle. *Circulation Research,* 70: 865-884, 1992.

Payne M.R. and S.E. Rudnick, Regulation of vertebrate striated muscle contraction. *Trends in Biochemical Sciences*, 14: 357-360, 1989.

Parry D.A.. and J. Squire, Time resolved X-ray diffraction studies of striated muscle *Molecular Biology*, 75: 33-55, 1973.

Patel J.R., G.A. Diffee and R.L. Moss, Myosin regulatory light chain modulates the calcium dependence on the kinetics of tension development in skeletal muscle fibers. *Biophysical Journal*, 70: 2333-2340, 1996.

Pemrick S.M., The phosphorylated LC2 of skeletal muscle is a modifier of the actomyosin ATPase. *Journal of Biological Chemistry*, 255: 8836-8841, 1980.

Potma E.J., I.A. Van Grass, and G.J.M. Stienen, Effects of pH on myofibrillar ATPase activity in fast and slow skeletal muscle fibers of the rabbit. *Biophysical Journal*, 67: 2404-2410, 1994.

Schutt C.E., and U. Lindberg, Actin as a generator of tension during muscle contraction. *Proceedings of the National Academy of Sciences*, Vol 89: 319-323, 1992.

Shephard R.J., *Physiology and Biochemistry of Exercise,* Praeger Publishers, 95-112, 1982

Staron R.S., and P. Johnson, Myosin phosphorylation and differential expression in adult human skeletal muscle. *Comparative Biochemistry and Physiology*, 106b: 463-475, 1993

Stein L.A., R. Scwartz, P.B. Chock, and E. Eisenberg, The mechanism of the actomyosin ATPase: evidence that ATP hydrolysis can occur without dissociation of the actomyosin complex. *Biochemistry,* 18: 3895-3909, 1979.

Steinen G.J.M., M.C.M. Roosemalen, M.G.A. Wilson, and G. Elzinga, Depression of force by phosphate in skinned skeletal muscle fibers of the frog. *American Journal of Physiology,* 259: C349-C357, 1990

Sweeny H.L. and J.T. Stull, Alteration of cross-bridge kinetics by myosin light chain phosphorylation in rabbit skeletal muscle: implications for regulation of actin-myosin interaction. *Proceedings of the National Academy of Sciences*, 87: 414-418, 1990.

Szent-Györgyi A., Free energy relations and contraction of actomyosin. *Biological Bulletin,* 96: 140, 1949

Westerblad H. and D.G. Allen, The contribution of [Ca]i to the slowing of relaxation in fatigued single fibers from mouse skeletal muscle. *Journal of Physiology*, 468: 729-740, 1993.

Williams J.H., C.W. Ward and G.A Klug., Fatigue induced alterations in Ca^{2+} and caffeine sensitivities of skinned muscle fibers. *Journal of Applied Physiology*, 75: 586-593, 1993

Williams, J.H. and C.W. Ward, Reduced Ca^{2+} induced Ca^{2+} release from skeletal muscle sarcoplasmic reticulum at low pH. *Canadian Journal of Physiology and Pharmacology,* 70: 926-930, 1992.

APPENDIX I
Solutions
Table 4

0.25 mM MgATP

pCa 9.0

	FW	Conc. (M)	g/250ml	HPr (ml/250ml)
CaO	56.08	0	0	0.0003
MgO	40.30	0.0015	0.015	0.0573
KOH	56.11	0.085	1.193	3.2035
EGTA	380.40	0.007	0.666	0.0000
Imidazole	68.08	0.1355	2.306	0.0000
HPr	74.08	0.077	1.427	1.4368

Total HPr	4.698
Water Added	245.302

pCa 4.5

	FW	Conc. (M)	g/250ml	HPr (ml/250ml)
CaO	56.08	0.0069	0.096	0.2585
MgO	40.30	0.0013	0.013	0.0474
KOH	56.11	0.085	1.193	3.2035
EGTA	380.40	0.007	0.666	0.0000
Imidazole	68.08	0.1354	2.305	0.0000
HPr	74.08	0.0638	1.181	1.1892

Total HPr	4.699
Water Added	245.302

Experimental solutions, 0.25mM MgATP
HPr = Propionic Acid

Table 5

0.5 mM MgATP

pCa 9.0

	FW	Conc. (M)	g/250ml	HPr (ml/250ml)
CaO	56.08	0.0000	0.000	0.0003
MgO	40.30	0.0031	0.031	0.1168
KOH	56.11	0.0850	1.193	3.2035
EGTA	380.40	0.0070	0.666	0.0000
Imidazole	68.08	0.1323	2.252	0.0000
HPr	74.08	0.0703	1.303	2.6501

Total HPr	5.971
Water Added	244.029

pCa 4.5

	FW	Conc. (M)	g/250ml	HPr (ml/250ml)
CaO	56.08	0.0066	0.093	0.2487
MgO	40.30	0.0030	0.030	0.1140
KOH	56.11	0.0850	1.193	3.2035
EGTA	380.40	0.0070	0.666	0.0000
Imidazole	68.08	0.1321	2.248	0.0000
HPr	74.08	0.0570	1.055	2.1472

Total HPr	5.713
Water Added	244.287

Experimental solutions, 0.5mM MgATP
HPr = Propionic Acid

Table 6

1.0 mM MgATP

pCa 9.0

	FW	Conc. (M)	g/250ml	HPr (ml/250ml)
CaO	56.08	0.000	0.0000	0.0000
MgO	40.30	0.023	0.023	0.8666
KOH	56.11	0.085	1.193	3.2026
EGTA	380.40	0.007	0.666	0.0000
Imidazole	68.08	0.134	2.279	0.0000
HPr	74.08	0.075	1.3815	2.8108

Total HPr	6.880
Water Added	243.120

pCa 4.5

	FW	Conc. (M)	g/250ml	HPr (ml/250ml)
CaO	56.08	0.007	0.096	0.2585
MgO	40.30	0.002	0.020	0.0760
KOH	56.11	0.085	1.193	3.2035
EGTA	380.40	0.007	0.666	0.0000
Imidazole	68.08	0.134	2.279	0.0000
HPr	74.08	0.061	1.135	1.1430

Total HPr	4.68
Water Added	245.32

Experimental solutions, 1.0mM MgATP
HPr = Propionic Acid

Table 7

2.0 mM MgATP

pCa 9.0

	FW	Conc. (M)	g/800ml	HPr (ml/800ml)
CaO	56.08	0.000	0.000	0.0009
MgO	40.3	0.003	0.106	0.3965
KOH	56.11	0.085	3.817	5.1256
EGTA	380.4	0.007	2.130	0.0000
Imidazole	68.08	0.132	7.206	0.0000
HPr	74.08	0.071	4.228	4.2575

Total HPr	9.780
Water Added	790.220

pCa 4.5

	FW	Conc. (M)	g/800ml	HPr (ml/800ml)
CaO	56.08	0.007	0.308	0.8271
MgO	40.30	0.003	0.098	0.3647
KOH	56.11	0.085	3.817	5.1256
EGTA	380.40	0.007	2.130	0.0000
Imidazole	68.08	0.132	7.195	0.0000
HPr	74.08	0.058	3.437	3.4610

Total HPr	9.778
Water Added	790.222

Experimental solutions, 2.0mM MgATP

HPr = Propionic Acid

Table 8

2.0mM MgATP, 10oC

pCa 9.0

	FW	Conc. (M)	g/800ml	HPr (ml/800ml)
CaO	56.08	0.000	0.000	0.0009
MgO	40.30	0.003	0.100	0.3738
KOH	56.11	0.085	3.817	5.1256
EGTA	380.40	0.007	2.130	0.0000
Imidazole	68.08	0.132	7.206	0.0000
HPr	74.08	0.070	4.166	4.1956

Total HPr	9.696
Water Added	790.304

pCa 4.5

	FW	Conc. (M)	g/800ml	HPr (ml/800ml)
CaO	56.08	0.0066	0.295	0.7919
MgO	40.30	0.0030	0.098	0.3647
KOH	56.11	0.0850	3.817	5.1256
EGTA	380.40	0.0070	2.130	0.0000
Imidazole	68.08	0.1321	7.195	0.0000
HPr	74.08	0.0569	3.369	3.3929

Total HPr	9.675
Water Added	790.325

Experimental solutions, 10° C

HPr = Propionic Acid

Table 9

2.0 mM MgATP, 15oC

pCa 9.0

	FW	Conc. (M)	g/800ml	HPr (ml/800ml)
CaO	56.08	0.0000	0.000	0.0009
MgO	40.30	0.0034	0.100	0.3738
KOH	56.11	0.0850	3.817	5.1256
EGTA	380.40	0.0070	2.130	0.0000
Imidazole	68.08	0.1323	7.206	0.0000
HPr	74.08	0.0703	4.166	4.1956

Total HPr	9.696
Water Added	790.304

pCa 4.5

	FW	Conc. (M)	g/800ml	HPr (ml/800ml)
CaO	56.08	0.0066	0.295	0.7919
MgO	40.30	0.0033	0.098	0.3654
KOH	56.11	0.0850	3.817	5.1256
EGTA	380.40	0.0070	2.130	0.0000
Imidazole	68.08	0.1321	7.195	0.0000
HPr	74.08	0.0569	3.369	3.3929

Total HPr	9.665
Water Added	790.345

Experimental solutions, 15° C

HPr = Propionic Acid

APPENDIX II

Gradient Calibration

Free Ca^{2+} concentrations with each pump step were periodically calibrated throughout the investigation using the fluorescent Ca^{2+} probe Calcium Green-2 (excitation = 480 nm, emission = 515). Fluorescence values were converted to free-Ca^{2+} from the relationship:

$$\text{Free } [Ca^{2+}] = k_d (F - F_{min}) / (F_{max} - F)$$

where F_{max} and F_{min} are the maximal and minimal fluorescence values recorded in the presence of 1mM free Ca^{2+} and 7mM EGTA, respectively. The k_d for Calcium Green-2 (k_d = 4.365μM) was provided by Dr. Glenn Kerrick. Results from a single calibration experiment are presented in Figure 17.

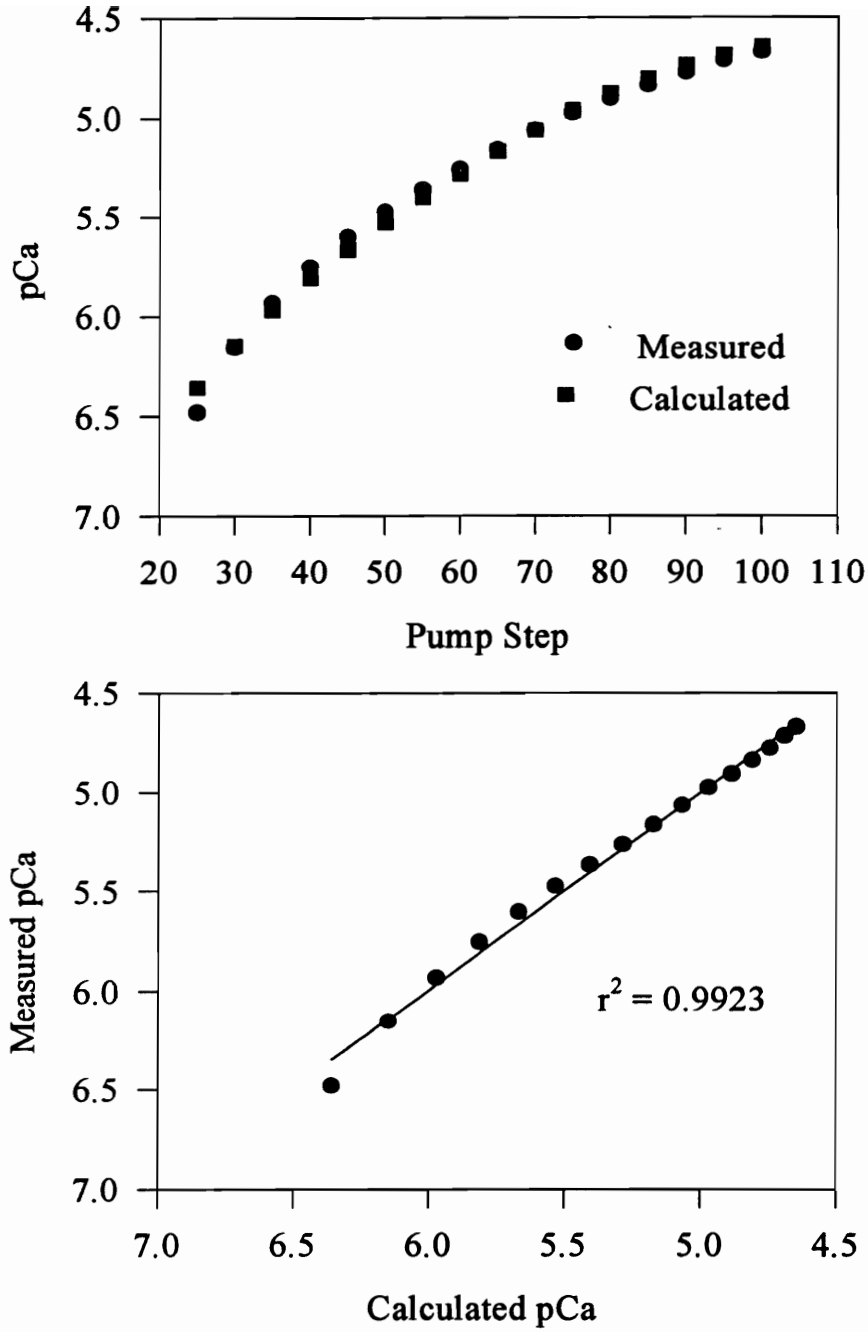

Figure 17. Calibration results from a single calibration procedure. Measured and calculated Ca^{2+}values vs. pump step (top). Measured pCa(-log[Ca^{2+}]) vs. calculated pCa (bottom).

APPENDIX III

Statistics

Table 10. Analysis of variance results. Comparison of $[Ca^{2+}]_{50}$ between conditions.

Source of Variance	DF	SS	MS
ATP	3	2.285	0.7618
ATP(FROG)	20	9.594	0.4797
MEAS	1	5.411	5.4111
ATP x MEAS	3	1.682	0.5607
Residual	20	0.821	0.0411
Total	47	21.459	0.4566

Source of Variance	F	P
ATP	1.59	0.2236
ATP(FROG)		
MEAS	131.75	<0.0001
ATP x MEAS	13.65	<0.0001
Residual		
Total		

MEAS = force or ATPase; ATP = 0.25, 0.5, 1.0 or 2.0mM MgATP; FROG = animal

Table 11. Analysis of variance results. Comparison of n between conditions.

Source of Variance	DF	SS	MS
ATP	3	3.916	1.305
ATP(FROG)	20	40.296	2.015
MEAS	1	44.904	44.904
ATP x MEAS	3	0.422	0.141
Residual	20	13.233	0.662
Total	47	105.653	2.248

Source of Variance	F	P
ATP	0.648	0.5935
ATP(FROG)		
MEAS	67.868	<0.0001
ATP x MEAS	0.213	0.8864
Residual		
Total		

MEAS = force or ATPase; ATP = 0.25, 0.5, 1.0 or 2.0mM MgATP; FROG = animal

Table 12. $[Ca^{2+}]_{50}$ of Force between Soleus and EDL fibers of the rat at 2.0 and 0.5 mM MgATP

Source of Variance	DF	SS	MS
Muscle	1	4.184	4.184
ATP	1	0.653	0.653
Muscle x ATP	1	3.711	3.711
Residual	24	9.693	0.404
Total	27	19.277	0.714

Source of Variance	F	P
Muscle	10.36	0.0037
ATP	1.62	0.2156
Muscle x ATP	9.19	0.0058
Residual		
Total		

Muscle = soleus or EDL; ATP= 2.0 or 0.5mM MgATP

Table 13. $[Ca^{2+}]_{50}$ of ATPase between Soleus and EDL fibers of the rat at 2.0 and 0.5 mM MgATP

Source of Variance	DF	SS	MS
Muscle	1	0.0136	0.0136
ATP	1	0.2249	0.2249
Muscle x ATP	1	0.8571	0.8571
Residual	24	5.4470	0.2270
Total	27	6.6027	0.2445

Source of Variance	F	P
Muscle	0.0599	0.8087
ATP	0.9910	0.3294
Muscle x ATP	3.7765	0.0638
Residual		
Total		

Muscle = soleus or EDL; ATP = 2.0 or 0.5mM MgATP

Table 14. $[Ca^{2+}]_{50}$ difference between force and ATPase between Soleus and EDL fibers of the rat at 2.0 and 0.5 mM MgATP

Source of Variance	DF	SS	MS
Muscle	1	3.720	3.720
ATP	1	0.112	0.112
Muscle x ATP	1	1.001	1.001
Residual	24	7.376	0.307
Total	27	12.798	0.474

Source of Variance	F	P
Muscle	12.105	0.0019
ATP	0.363	0.5524
Muscle x ATP	3.257	0.0837
Residual		
Total		

Muscle = soleus or EDL; ATP = 2.0 or 0.5mM MgATP

APPENDIX IV

Raw Data

Rat EDL Fibers 2.0mM [ATP]

	Force			ATPase Activity				
	[Ca]50 (μM)	n	pCa50	A (μM/s)	(h-1·s-1)	[Ca]50 (μM)	n	pCa50
1	3.591	3.778	5.44	639.41	4.15	1.256	2.668	5.90
2	2.646	3.309	5.58	321.86	2.09	1.129	2.988	5.95
3	2.076	4.603	5.68	434.28	2.82	1.656	5.074	5.78
4	3.540	3.365	5.45	463.54	3.01	1.115	2.045	5.95
5	2.160	3.302	5.67	645.26	4.19	1.094	2.268	5.96
6	3.730	4.416	5.43	355.74	2.31	2.427	3.775	5.61
7	3.402	4.994	5.47	343.42	2.23	2.547	4.199	5.59
Mean	3.02071	3.967	5.52	457.644	2.972	1.6034	3.2881	5.79
SEM	0.26802	0.264		51.336	0.333	0.2398	0.4174	

Rat EDL Fibers 0.5 mM [ATP]

	Force			ATPase Activity				
	[Ca]50 (μM)	n	pCa50	A (μM/s)	(h-1·s-1)	[Ca]50 (μM)	n	pCa50
1	2.077	4.440	5.68	151.44	0.98	1.476	1.540	5.83
2	1.369	4.217	5.86	237.68	1.54	1.214	2.993	5.92
3	1.653	2.602	5.78	60.24	0.39	0.908	1.362	6.04
4	0.978	7.901	6.01	107.08	0.70	0.985	2.169	6.01
5	2.130	3.593	5.67	106.15	0.69	0.960	1.394	6.02
Mean	1.6413	4.551	5.802	132.518	0.860	1.1086	1.8915	5.96
SEM	0.2172	0.896		29.986	0.194	0.1057	0.3116	

Rat Soleus Fibers 2.0mM [ATP]

	Force			ATPase Activity				
	[Ca]50 (μM)	n	pCa50	A (μM/s)	(h-1·s-1)	[Ca]50 (μM)	n	pCa50
1	0.894	3.336	6.05	203.28	1.32	0.665	2.372	6.18
2	0.918	2.407	6.04	240.24	1.56	0.717	2.617	6.14
3	2.134	3.435	5.67	189.42	1.23	1.990	2.624	5.70
4	0.880	2.333	6.06	206.36	1.34	0.670	2.772	6.17
5	1.812	2.462	5.74	221.76	1.44	1.075	2.742	5.97
6	1.831	2.846	5.74	212.83	1.38	1.590	2.343	5.80
7	1.839	3.154	5.74	224.84	1.46	1.617	1.582	5.79
8	1.166	3.258	5.93	226.07	1.47	0.946	1.997	6.02
9	1.905	3.995	5.72	249.48	1.62	1.537	1.939	5.81
Mean	1.4864	3.025	5.83	219.364	1.424	1.2007	2.3320	5.92
SEM	0.1703	0.186		6.226	0.040	0.1644	0.1374	

Rat Soleus Fibers 0.5mM [ATP]

	Force			ATPase Activity				
	[Ca]50 (μM)	n	pCa50	A (μM/s)	(h-1·s-1)	[Ca]50 (μM)	n	pCa50
1	1.860	3.620	5.73	91.78	0.6	1.770	2.490	5.75
2	1.710	3.070	5.77	213.45	1.39	1.480	1.990	5.83
3	2.060	3.670	5.69	59.08	0.39	1.840	1.390	5.74
4	1.520	3.350	5.82	67.58	0.44	0.845	1.504	6.07
5	1.430	3.430	5.84	75.67	0.49	0.941	1.322	6.03
Mean	1.7160	3.428	5.77	101.512	0.662	1.3752	1.7392	5.88
SEM	0.1139	0.107		28.500	0.185	0.2065	0.2211	

Mouse EDL Fibers

	Force				ATPase Activity			
	[Ca]50 (μM)	n	pCa50	A (μM/s)	(h-1·s-1)	[Ca]50 (μM)	n	pCa50
1	2.25	4.00	5.65	766.92	4.98	0.98	2.98	6.01
2	2.06	3.98	5.69	666.82	4.33	0.97	3.00	6.01
3	2.19	4.23	5.66	773.08	5.02	1.05	3.11	5.98
4	1.99	4.51	5.70	1033.34	6.71	1.11	2.88	5.95
5	2.23	4.02	5.65	907.06	5.89	0.98	2.56	6.01
6	2.05	4.11	5.69	888.58	5.77	1.09	2.65	5.96
7	2.13	4.01	5.67	766.92	4.98	0.89	3.05	6.05
8	2.20	3.89	5.66	803.88	5.22	1.13	2.88	5.95
9	2.08	4.35	5.68	773.08	5.02	1.03	2.56	5.99
10	2.13	4.26	5.67	1059.52	6.88	1.09	2.31	5.96
Mean	2.131	4.136	5.672	843.920	5.480	1.032	2.798	5.987
SEM	0.027	0.062		39.890	0.259	0.024	0.083	

Frog ST Fibers 2.0mM [ATP]

	Force				ATPase Activity			
	[Ca]50 (μM)	n	pCa50	A (μM/s)	(h-1·s-1)	[Ca]50 (μM)	n	pCa50
1	2.909	4.81	5.54	307.70	2.00	1.586	2.433	5.80
2	2.025	7.409	5.69	308.00	2.06	1.43	4.29	5.84
3	3.407	4.788	5.47	282.61	1.84	2.147	2.73	5.67
4	2.815	3.781	5.55	261.82	1.70	1.596	2.864	5.80
5	2.144	5.041	5.67	481.84	3.31	1.443	3.074	5.84
6	2.665	3.48	5.57	784.98	5.10	1.752	2.395	5.76
7	2.334	5.257	5.63	562.31	3.65	1.415	3.339	5.85
8	2.79	2.705	5.55	389.63	2.53	1.636	1.924	5.79
9	2.701	5.3695	5.57	398.17	2.59	1.273	2.565	5.90
Mean	2.644	4.738	5.583	419.673	2.753	1.586	2.846	5.804
SEM	0.141	0.449		56.241	0.367	0.085	0.227	

Frog ST Fibers 1.0mM [ATP]

	Force			ATPase Activity				
	[Ca]50 (μM)	n	pCa50	A (μM/s)	(h-1·s-1)	[Ca]50 (μM)	n	pCa50
1	2.774	3.97	5.56	277.02	1.80	1.308	2.002	5.88
2	2.117	3.693	5.67	239.46	1.55	1.183	2.21	5.93
3	2.024	3.928	5.69	222.06	1.44	1.409	2.195	5.85
5	2.571	4.592	5.59	253.57	1.65	1.26	1.815	5.90
6	2.63	5.652	5.58	222.51	1.44	1.325	1.976	5.88
Mean	2.423	4.367	5.619	242.924	1.576	1.297	2.039	5.888
SEM	0.148	0.354		10.344	0.068	0.037	0.074	

Frog ST Fibers 0.5mM [ATP]

	Force			ATPase Activity				
	[Ca]50 (μM)	n	pCa50	A (μM/s)	(h-1·s-1)	[Ca]50 (μM)	n	pCa50
1	1.134	2.77	5.95	93.38	0.61	0.774	2.296	6.11
2	2.996	3.55	5.52	100.48	0.65	3.035	2.44	5.52
3	1.601	5.508	5.80	99.88	0.65	1.007	2.199	6.00
4	1.43	2.237	5.84	162.17	1.05	0.975	2.511	6.01
5	2.333	5.795	5.63	104.00	0.68	1.796	3.894	5.75
6	1.701	5.509	5.77	87.03	0.57	1.184	3.249	5.93
Mean	1.866	4.228	5.752	107.823	0.702	1.462	2.765	5.885
SEM	0.278	0.640		11.145	0.071	0.345	0.272	

Frog ST Fibers 0.25mM [ATP]

	Force			ATPase Activity				
	[Ca]50 (μM)	n	pCa50	A (μM/s)	(h-1·s-1)	[Ca]50 (μM)	n	pCa50
1	1.149	6.46	5.94	35.27	0.23	1.043	3.172	5.98
2	2.555	3.085	5.59	50.56	0.33	2.032	1.575	5.69
3	1.726	3.111	5.76	67.57	0.44	1.804	1.696	5.74
4	1.299	3.969	5.89	86.97	0.56	0.961	2.042	6.02
5	0.9957	2.399	6.00	72.49	0.47	1.178	1.386	5.93
Mean	1.545	3.805	5.837	62.572	0.406	1.460	2.121	5.859
SEM	0.280	0.709		8.967	0.057	0.216	0.318	

VITA

Christopher William Ward was born in Miami, Florida on November 28, 1967 and was adopted by William and Virginia Ward on December 20 of that year. The rest of his immediate family includes his adopted sister LoriAnn, her husband Lewis, and new niece Ansley Virginia.

Chris enrolled at Virginia Tech as an undergraduate student and earned a B.S.(1989) and M.S. (1991) in Exercise Physiology. In 1993 he returned to pursue a doctoral degree in physiology at the Virginia/Maryland Regional College of Veterinary Medicine in which he pursued his interests in the area of muscle physiology.

In his tenure at VMRCVM Chris has had two terms as a teaching assistant, has been a member of VMRCVM and University committees, and has pursued hobbies which include SCUBA diving and Golf.

For the coming year Chris has accepted a 1 year appointment as a Visiting Assistant Professor in the College of Human Nutrition and Foods. He plans to dedicate any free time in the coming year to learning how to play the guitar.